Master's thesis

NTNU
Norwegian University of Science and Technology
Faculty of Information Technology and Electrical Engineering
Department of Electric Power Engineering

Line Nyegaard

Multi-Period AC Optimal Power Flow for Distribution Systems with Energy Storage

Master's thesis in Energy and Environmental Engineering
Supervisor: Vijay Venu Vadlamudi
June 2019

NTNU
Norwegian University of Science and Technology

Line Nyegaard

Multi-Period AC Optimal Power Flow for Distribution Systems with Energy Storage

Master's thesis in Energy and Environmental Engineering
Supervisor: Vijay Venu Vadlamudi
June 2019

Norwegian University of Science and Technology
Faculty of Information Technology and Electrical Engineering
Department of Electric Power Engineering

NTNU
Norwegian University of
Science and Technology

Abstract

Battery energy storage systems are increasingly considered as a flexible resource in the power system providing a wide range of technical, economic, and environmental advantages. Deployed in the distribution grid, as a community energy storage (CES), the unit can have multiple purposes. It can prevent congestion problems on the network by participating during peak consumption hours, resulting in local energy balance. Besides, it can facilitate a higher amount of renewable generation. The integration of decentralized renewable production is increasing and must continue to rise for the world to achieve a more sustainable power system. However, renewable energy sources are generally unregulated and have a low contribution to power flexibility. Thus, the need for balancing service will become critical in operating the future power system.

In planning and operating of the power system, Optimal Power Flow (OPF) has an undeniable role as a technical and economical tool. Broadly speaking, the OPF optimizes the power system operation according to an objective while meeting all system constraints, including the power flow equations. In line with technological developments and trends in the power system, there is a need for new models and solution methods for the OPF problem. The increasing deployment of energy storage requires that the OPF captures the couplings between different time-steps that are introduced, giving rise to multi-period AC OPF.

This thesis work is emphasizing on providing pedagogical clarity of the fundamental and methodological aspects of multi-period AC OPF. A literature survey is conducted with the purpose of elucidating the current state of research on the relevant study. The aim of this master has also been to create a multi-period AC OPF model. The model is tested on various test-systems. The case studies have been kept simple and illustrative with the purpose of showing the characteristics of system operation strategy when energy storage is deployed. Another intention of the case studies is to demonstrate some applications that can be performed by the proposed solution strategy. From the thesis work, it has become evident that multi-period AC OPF has proved to be a powerful tool in power system analyzing when optimization over a time horizon is favorable.

Sammendrag

Batterilagringssystemer blir i økende grad betraktet som en fleksibel ressurs i kraftsystemet, ettersom lagringsenheten har mulighet til å tilby et bredt spekter av tekniske, økonomiske og miljømessige fordeler. I distribusjonssystemet kan batterier forhindre overbelastning på linjer ved å lagre energi til fremtidig bruk, dette bidrar til lokal energibalanse. Lagringsenheten kan også legge til rette for en økende integrering av fornybare energikilder i nettet. Mengden av elektrisitetsproduksjon fra desentraliserte fornybar kilder øker, og må fortsette å stige for at verden skal oppnå mer bærekraftig kraftproduksjon. Det er en utfordring at fornybare energikilder er ikke-regulerbare og i liten grad bidrar til fleksibilitet i kraftnettet. Behovet for en balansetjeneste blir derfor avgjørende i driften av det fremtidige kraftsystemet.

Optimal Power Flow (OPF) er et viktig teknisk og økonomisk verktøy i planlegging og drift av kraftsystemet. OPF optimaliserer kraftsystemet i henhold til en objektivfunksjon samtidig som systembegrensninger opprettholdes. I tråd med den teknologiske utviklingen og trender i kraftsystemet er det behov for nye modeller og løsningsmetoder på OPF-problemet. Utplassering av lagringsenheter i distribusjonssystemet beskriver en slik trend, og gir opphav til multi-period AC OPF.

Denne oppgaven legger vekt på å gi en pedagogisk introduksjon til grunnleggende teori og metodiske aspekter ved multi-period AC OPF. En litteraturundersøkelse er gjennomført med det formål å belyse nåværende forskning publisert om emnet. Et av målene med masteroppgaven har vært å utvikle en multi-period AC OPF modell, implementere denne i MATLAB og teste den på ulike systemer. Studiene er holdt enkle og illustrerende, og har som formål å vise hvordan kraftsystemet operer over tid når et batteri er inkludert. En annen hensikt med studiene er å demonstrere noen applikasjoner som kan utføres med den foreslåtte strategien. Multi-period AC OPF har vist seg å være et kraftig verktøy i analyse av kraftsystemet når optimering over en tidshorisont er gunstig.

Preface

This Master Thesis has been written at the Department of Electric Power Engineering and concludes my education at the Norwegian University of Science and Technology (NTNU). The last five years have been wonderful, and I am forever grateful for the experiences I have gained as a student.

The thesis gives an introduction to multi-period AC OPF, with an emphasis on providing pedagogical clarity of the fundamentals. I extend my sincerest gratitude to my supervisor, Vijay Venu Vadlamudi, your support and guidance have been invaluable. You have always been available and encouraged me in my endeavors.

I would also like to thank Ph.D. candidate Salman Zaferanlouei for helping me with the modeling in MATLAB. Without your help, this work would never have come to fruition.

Lastly, I would like to express gratitude towards my friends and family for all your love and support. A special thank you is aimed at fellow students who have provided interesting discussions and an excellent working environment.

Trondheim, June 2019
Line Nyegaard

Table of Contents

Abstract **i**

Sammendrag **iii**

Preface **v**

Table of Contents **ix**

List of Figures **xii**

Abbreviations **xiii**

1 Introduction **1**

1.1 Motivation 1

1.2 Contributions 2

1.3 Structure of Thesis 3

2 Envisioned Future Distribution System **5**

2.1 Distribution System Characteristics 5

2.1.1 Regulation of Quality of Supply 7

2.2 Decentralized Renewable Generation 7

2.3 The Norwegian Load Pattern 8

2.4 Energy Storage in the Distribution Grid 9

3 Conceptual Background **13**

3.1 Power System Analysis . . . 13
3.2 Optimal Power Flow . . . 17
3.2.1 Variables . . . 17
3.2.2 Constraints . . . 18
3.2.3 Objective Function . . . 19
3.3 Multi-Period Optimal Power Flow . . . 20
3.4 Optimization Methods . . . 22
3.4.1 The Interior Point Algorithm of `fmincon` . . . 23

4 Literature Review **25**
4.1 Optimal Power Flow in Literature . . . 25
4.2 Survey of Multi-Period AC OPF Methods . . . 26
4.2.1 Formulation of the Objective Function . . . 30
4.2.2 Formulation of the Energy Storage Balance Equation . . . 31

5 General Methodology and Modeling in MATLAB **33**
5.1 Optimization Problem Formulation . . . 33
5.1.1 Assumptions . . . 33
5.1.2 Notation . . . 34
5.1.3 Mathematical Model . . . 34
5.1.4 Model Formulation . . . 38
5.2 Modelling in MATLAB . . . 38
5.3 Illustrative Example . . . 41
5.3.1 3-Bus Test System . . . 41
5.3.2 Model . . . 41

6 Cases and Implementation **51**
6.1 3-Bus Test System . . . 51
6.2 Modified IEEE 9-Bus System . . . 53
6.3 Radial 9-Bus System . . . 57
6.4 Implementation . . . 59
6.4.1 Implementation of Non-Linear Constraints . . . 60

7 Case Studies **63**

7.1 3-Bus Test System 63

7.1.1 Discussion 67

7.2 Modified IEEE 9-Bus System 67

7.2.1 Discussion 70

7.3 Radial 9-Bus System 70

7.3.1 Case: Quadratic Cost-Function 70

7.3.2 Case: Time-Variable Cost-Function 72

7.3.3 Discussion 73

7.4 Discussion of Case Studies 73

8 Conclusion and Further Work **75**

8.1 Conclusion 75

8.2 Further Work 78

Bibliography **78**

A Formula: Voltage drop **85**

B MATLAB code **87**

B.1 3-Bus Test System 87

List of Figures

2.1 Conventional two-bus distribution system showing the voltage drop between two buses 6
2.2 Solar PV global capacity and annual additions, 2007-2017 8
2.3 Spot price for Oslo May 24th 2019 9
2.4 Characteristic time scale of energy storage applications. 10

3.1 Illustrating the idea of a multi-period OPF model 22

4.1 Survey of multi-period AC OPF 29

5.1 Illustration of 3-bus test system 41

6.1 Total system load hour by hour 52
6.2 Modified IEEE 9-bus system 53
6.3 Total system load hour by hour 54
6.4 PV generation hour by hour 55
6.5 Radial 9-bus test system 57
6.6 Total system load hour by hour 58
6.7 PV generation hour by hour 59
6.8 AC OPF architectural flowchart 60

7.1 Objective functions plotted against power generation on the x-axis 64
7.2 Operation strategy with objective function formulated as a minimizing constant cost-function (a) 65

7.3 Operation strategy with objective function formulated as a minimizing quadratic cost-function (b) 66
7.4 Operation strategy with objective function formulated as a minimizing time-varying cost-function (c) 66
7.5 Results from the multi-period AC OPF simulation depicting hourly operation strategy 68
7.6 Hour by hour generation with and without BESS installed in the system 69
7.7 Results from the multi-period AC OPF simulation depicting hourly operation strategy with quadratic cost-function 71
7.8 Results from the multi-period AC OPF simulation depicting hourly operation strategy with time-variable cost-function. Spot prices for Oslo, May 24th 2019. Data retrieved from NordPool 72

Abbreviations

AC	Alternating Current
BESS	Battery Energy Storage System
CES	Community Energy Storage
DC	Direct Current
DER	Decentralized Energy Resources
DG	Distributed Generation
DOPF	Dynamic Optimal Power Flow
DSO	Distribution System Operator
ESS	Energy Storage System
EV	Electric vehicle
LHS	Left-Hand Side
LMP	Locational Marginal Pricing
LV	Low Voltage
MV	Medium Voltage
NR	Newton Ralphson
OPF	Optimal Power Flow
PF	Power Flow
PCC	Point of Common Coupling
PV	Photovoltaics
RE	Renewable Energy
RES	Renewable Energy Source
RHS	Right-Hand Side
RMS	Root Mean Square
SCR	Short Circuit Ratio

Chapter 1

Introduction

1.1 Motivation

The power sector is going through a tremendous transformation, and the way we generate, transport, store, and use energy is changing. The complexity of the system is increasing owing to a number of reasons, such as more significant uncertainty caused by the adoption of renewable generation, changes in consumption patterns including a higher peak demand and deregulation of electricity markets [1]. Deployment of battery energy storage systems (BESS) is increasingly considered for several applications in the power system, as it can provide a wide range of technical, economic, and environmental advantages [2].

Optimal Power Flow is a large class of optimization problems, with the intention of determining the optimal operating state of a power system while upholding all constraints imposed by electrical laws and limits on variables [3]. It is an important technical and economical tool and has an undeniable role in the planning and operation of electric power systems. In line with technological and economic developments, there is a great need for finding new ways of analyzing the power system. One of these technological developments is the inclusion of energy storage systems in the distribution grid [4].

When introducing energy storage in the power system, we are allowing for energy to be stored at one point in time and dispatched at later times. Thus, a coupling between time-steps is created. From the perspective of optimal power flow, the presence of storage requires that the model capture these dependencies. The correlation is presence thorough inter-temporal [1]

[1] Inter-temporal: "Describing any relationship between past, present and future events or conditions" [5]

constraints, making it unfavorable to consider each time-step in isolation as in conventionally done in OPF [4]. To accurately capture the time-coupling, we need to perform the optimization over several periods within the horizon simultaneously.

Furthermore, when studying energy storage systems deployed in the distribution grid, one must have in mind that the low voltage levels are quite susceptible to changes in operating conditions [6]. With the increasing integration of intermittent and decentralized renewable generation, more disturbance is also introduced in the distribution grid. Hence, it is desirable to capture voltage violations and system instability when evaluating the system through OPF analysis. To do so, one generally has to include the full alternating current (AC) representation of the power flow equations in the OPF model. Accordingly, this thesis work is investigating the field of multi-period AC OPF, including energy storage and distributed generation (DG).

1.2 Contributions

The topic of multi-period optimal power flow has in later years received increasing attention, and it is published a great amount of work on the subject. However, none of the work studied has emphasized providing a pedagogical clarity of the fundamentals and methodological aspects of multi-period AC OPF. I light of the shortcomings mentioned above, this thesis aims to provide the following contributions:

- Giving a brief introduction to the fundamental theoretical concepts required to understand the structure of a multi-period AC OPF model.
- Conducting a literature survey to elucidate the current state of research on multi-period AC OPF problems. By investigating previous publications, the goal is to provide a closer insight into a selected-few representative methodologies from the literature.
- Presenting an optimization model including general assumptions with the objective of minimizing generation cost. After that, give a clear explanation of how the model is implemented in commercial software. More specifically `fmicon`, which is a built-in optimization solver in MATLAB Optimization Toolbox.
- Conducting case studies with the underlying goal of illustrating that the multi-period AC OPF structure presented in the thesis can be successful in producing the optimal operation

strategy of a system when energy storage is deployed.

1.3 Structure of Thesis

Chapter 1 - *Introduction*, provides the motivational background followed by a formulation of the contributions of the thesis work.

Chapter 2 - *Envisioned Future Distribution System*, gives a presentation of the system characteristics and developments in distribution systems.

Chapter 3 - *Conceptual Background*, present a brief introduction of the mathematical concepts behind a multi-period AC OPF model.

Chapter 4 - *Literature Review*, presents a survey of existing research on multi-period AC OPF. The papers investigated are compared in terms of methodologies, objective function, and constraints.

Chapter 5 - *General Methodology and modeling in MATLAB*, introduces a multi-period AC OPF model, and give a pedagogical explanation of the implementation using MATLAB.

Chapter 6 - *Case Study and Implementation*, introduce the test systems studied in the thesis, and provide a qualitative description of the computational procedure.

Chapter 7 - *Case studies*, contain the main results obtained from simulation along with a brief discussion of the observations.

Chapter 8 - *Conclusion and Further Work*, summarizes and concludes the main aspects of the study, along with suggestions for further work.

Parts of the content from chapters 2 and 3 is a replication of the specialization project work, with suitable extensions where deemed necessary.

Chapter 2

Envisioned Future Distribution System

The present distribution system is gradually trending towards a smart paradigm defined by developments within decentralized energy resources (RES), advanced power electronics and information and communications technology [7]. Such a profound transformation brings significant opportunities but also introduces new challenges for the distribution system operator (DSO).

This chapter starts by pointing out the physical characteristics of the distribution system that are influencing the mathematical modeling. Further, some of the trends in distribution system evolution are described more in detail. And finally, energy storage systems are introduced, and possible applications are mentioned.

2.1 Distribution System Characteristics

In order to understand the challenges related to changes appearing in the distribution grid, some of the characteristics of the network that differ from the transmission grid must be pointed out.

- The system is operated at low (230V or 400V) to medium (11kV or 22kV) voltage levels (LV/MV)
- The X/R-ratio is low
- Lines/radials are possible long and stretching over large areas
- Weak grid

The distribution grid radials are often described as weak [6]. A weak grid can be defined as a network that is more susceptible to changes in operating conditions. Whereas a stronger

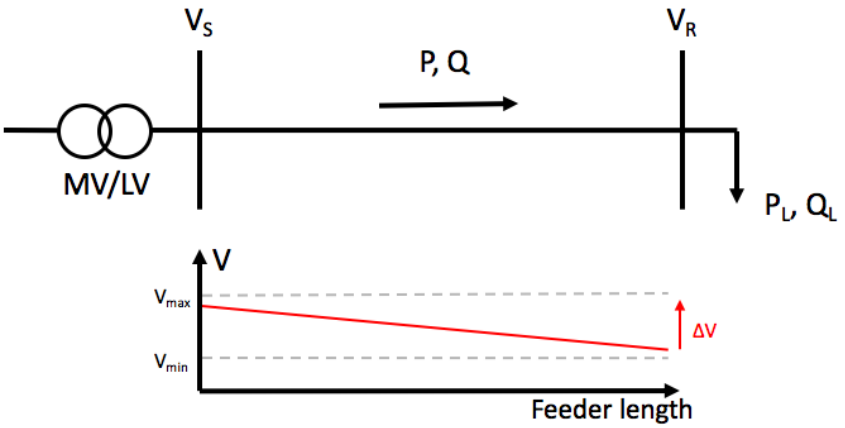

Figure 2.1: Conventional two-bus distribution system showing the voltage drop between two buses

network has a higher capability to withstand changes in operating conditions, hence the voltage level is more or less constant. The strength of the grid can be indicated by calculating the short circuit ratio (SCR), as shown in equation (2.1). Low values of SCR can characterize a weak grid. It must be mentioned that the SCR does not indicate the strength of an entire system, but the strength at a specific point in the system [8]. As noticeable from the eq. (2.1), another characteristic of a weak grid, is high impedance.

$$SCR = \frac{V_{\mathrm{PCC,nom}}^2}{Z_{\mathrm{tot}} S_{\mathrm{nom}}} \tag{2.1}$$

Studying a conventional two-bus system as depicted in fig. 2.1. V_{S} and V_{R} are the voltages at sending and receiving end respectively, P and Q are the real and reactive power flowing between the two buses and P_{L} and Q_{L} are the real and reactive load demand. The voltage drop in the radial is illustrated in the figure, and it is noticeable that the voltage stays within the allowable range. The approximation of the voltage drop in the radial is given as below

$$\Delta V \approx \frac{RP + XQ}{V_{\mathrm{s}}} \tag{2.2}$$

Assuming the angle between the sending and receiving end to be small [9]. The total derivation of the formula is given in Appendix A. The formula indicates that the longer the radials are, the more significant is the voltage drop. It is also noticeable that the impedance will impact the change in voltage magnitude. It is observable that the ratio of X/R indicates which values that are affecting the voltage variation [9]. For a distribution grid, relative to a transmission grid, the value of R is large. This is due to physical line data, which is not explained further in this

work. Consequently, changes in real power will influence the voltage magnitude more. This is also noticeable through the power flow equations, as described in section 3.1.

2.1.1 Regulation of Quality of Supply

The distribution system is constructed to operate as a balanced three-phase system i.e., sinusoidal voltages having the same amplitude but dispatched in phase by $120°$ [10]. In reality, this is not the case. The penetration of renewable sources, unbalanced loads, and power electronics resulting in more harmonics are all introducing disturbances to the grid. Poor power quality can harm system components and consumer equipment resulting in overheating of transformers and faulty operation of heat pumps, for instance. To ensure a satisfactory quality of supply, there exist both national and international regulations. In Norway, the "Regulation of Quality of Supply in the Electric Power Grid" describes requirements when it comes to the reliability of supply and voltage quality [11]. Voltage magnitude is one of the parameters that must be kept within a narrow range. According to the regulation, for low voltage grids, slow variations of the RMS voltage should not exceed $\pm 10\%$ of the nominal value. The voltage is measured at a connection point between supplier and consumer during one minute.

2.2 Decentralized Renewable Generation

Renewable and decentralized energy resources are widely adopted in distribution systems throughout the world. Take photovoltaic (PV) as an example. The installed capacity has escalated over the past years, as seen in fig. 2.2. In 2017 the recorded increase in generation was 34%, and the growth is assumed to continue [12]. The installation of PV panels is rapidly increasing also in Norway. A study completed by Multiconsult and Asplan Viak [13], reveals that there was a 59% growth in installation from 2016 to 2017.

The strongest motivator for the increasing amount of installation are the environmental advantages [14]. Other contributions are economical and technological incentives, as the costs are decreasing and the technology is developing. Distributed generation close to the consumer provides many advantages such as reduction of line losses, improvement in power quality, and reliability improvements [15].

Integrating renewable energy resources (RES) in the low voltage distribution system also in-

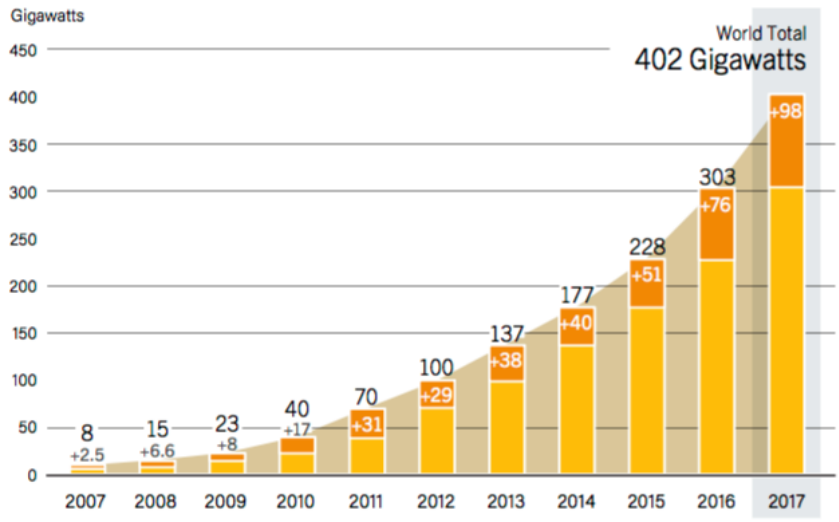

Figure 2.2: Solar PV global capacity and annual additions, 2007-2017 [17]

troduces significant challenges for the grid operators. In general, the issues are characterized by making the system unpredictable and unstable. This is mainly a result of the non-dispatchable character resulting in a volatile production and that the distribution system is not designed for power to be injected (see sec. 2.1). With significant penetration of DG, some unwanted effects are violations of thermal ratings of equipment, power quality problems, and reverse power flow [16].

2.3 The Norwegian Load Pattern

The energy consumption from private consumers varies over the course of a day. The common trend is if following a curve with one peak in the morning and another in the afternoon. This can be reflected in the hourly electricity price, as a higher price is usually the result of higher consumption. Figure 2.3 show the variation in price over a day in May for Oslo. It is noticeable that the price is considerably higher in the morning and afternoon.

Even though the peak-demand appears for a short duration of time, the power grid must be dimensioned to cover this demand. Moreover, the network must be able to cope with the highest peak-hour, even though it may only occur for a couple of hours a year. With the electrification of society, especially within the transport sector, the consumption patterns are characterized by even higher peak demand hours. Due to the increasing consumer load demand and the need for upgrading weak, old parts of the grid, the grid companies in Norway are expected to invest

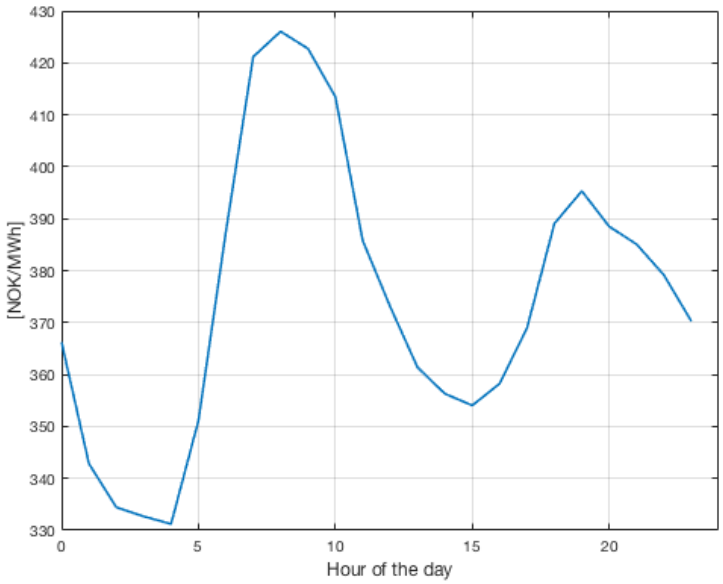

Figure 2.3: Spot price for Oslo May 24th 2019 [18]

heavily in the network in the future [19]. The consumers will pay this added cost through higher grid tariffs.

The grid companies are looking for new ways to solve this challenge. According to THEMA Consulting Group,[19], four primary resources can offer local flexibility: the grid, production, demand response, and storage. Energy storage systems as a source of flexibility is further investigated in this thesis work.

2.4 Energy Storage in the Distribution Grid

Energy storage systems can provide a wide range of technical, economic, and environmental advantages [20, 21]. And will, therefore, play an important role as a flexible distributed energy source in the optimal operation and planning of future systems. ESS can cover a wide range of applications in the distribution grid where variations range from a few weeks to fluctuations within seconds [14]. An overview of applications is given in fig. 2.4. The scope of this work is limited to focus on batteries, but other storage technologies embedded can provide the same improvements to the distribution grid. There exist several types of battery technology depending on size and location [22]. Much literature has focused on a distributed small scale and prosumer owned storage or large scale utility-owned storage. This work is studying community energy

Figure 2.4: Characteristic time scale of energy storage applications. Inspired by [23]

storage (CES), which is installed in a residential area. CES can perform several applications with a positive impact for both the grid operators and end users. A battery is representing a versatile type of energy storage as it can act as a generator, an integrated part of the grid or as a load with a high degree of flexibility [14]. One of the major advantages compared to other storage technologies is the ability to provide a rapid charging/discharging scheme as well as being flexible when it comes to placement. Network violations, like thermal overloading of lines or equipment, have traditionally been avoided by system expansions. Due to developments in technology and decreasing costs, batteries are becoming a competitive alternative to traditional grid investments.

A storage unit installed in a local community can help reduce the strain on the grid during peak-hours by storing energy at times of low demand and deliver power to the grid when the load is high. Thus, be used for peak shaving and valley filling, resulting in local energy balance. The upgrading of the network can then be postponed or at least upgraded to a smaller capacity. Additionally, by flattening out the generation profile, the cost of electricity may decrease as production is shifted from times of high cost to times of low cost. If there is decentralized energy resources in the grid, the storage can also facilitate a higher amount of renewable production by storing energy at times when production exceeds demand. The above mentioned operating functions are studied more in detail through the case studies in chapter 7.

A community energy storage can also provide several other benefits, these are not further investigated in this thesis but mentioned below. By storing energy in times of high feed-in, the storage also reduces the possibility for reversed power flow resulting in less stress on overlying grids [24]. For short duration requirements, storage can be used for network services like volt-

age and frequency control support. The fluctuating feed-in caused by RES and the increasing amount of fast chargers for electrical vehicles (EV) with a frequent on/off switch on the demand side, results in a growing demand for voltage regulation [14]. The deployment of energy storage in the distribution grid can be a significant avenue for maximizing energy efficiency, and the overall network performance can be enhanced [21].

Chapter 3

Conceptual Background

This chapter gives a brief presentation of the fundamental theoretical concepts required to understand the structure of a multi-period AC OPF model. Thus, the first section, 3.1, introduces the basics of Power System Analysis. Further, the mathematical concepts behind Optimal Power Flow and Multi-Period OPF is given in 3.2 and 3.3. The chapter ends with introducing the algorithm chosen to solve the non-linear problem.

3.1 Power System Analysis

The following section will present the basics of Power System Analysis and conventional Power Flow (PF), much inspired by [10] and [25]. In PF analysis, we are studying the power system during steady-state operation and the system is assumed to be underbalanced conditions. The power flow solution vector is expressing the state of the system and contains the unknown state variables. From this information, we may compute the active- and reactive power flow in each branch. The information obtained from the study is essential for operating the power system and for planning future expansions.

A power system consists of a large number of buses interconnected by branches. Each bus is characterized by four variables, P_i, Q_i, $|V_i|$ and δ_i, of which two are specified, and the other two must be calculated. Depending on which variables are specified, the buses can be classified to one of the following categories:

- **Slack bus:** Voltage magnitude and phase angle are fixed, the slack bus is chosen as a reference point such that all bus voltages are uniquely determined. The slack bus also

ensures a balance between generation and load demand.

- **Load bus:** Active and reactive power injections are specified, while the magnitude and phase angle of voltage are unknown variables to be determined. Load buses are also called P-Q buses.

- **Generator bus:** Active power injection and voltage magnitude are fixed, while reactive power injections and voltage angle are unknown and must be determined in the analysis. Generator buses are also called P-V buses.

When developing the power flow equations, we need to consider the network typology and characteristics of the lines and components. As there exist several ways of representing the typology, a choice regarding how the network model is expressed must be made. There exist two commonly used network models, the bus injection model, and the branch flow model [26]. The bus injection model represents the system in terms of nodal variables i.e., active and reactive power injections, voltage, and current injections at each bus. Historically, this has been the most widely used network model. Instead of basing the modeling on nodal variables, the branch flow model represents the system in terms of currents and power flows through the lines. More recent research has aroused interest in the branch flow model due to its advantages regarding convex relaxation of OPF problems [26, 27]. In this thesis, the power flow equations are derived from the bus injection model.

We begin by defining the admittance matrix, Y_{bus}, which is describing the network typology by summing up the admittances between all interconnected buses in the system. The self admittance of each bus is placed along the diagonal and the admittance value between buses on the off-diagonal.

$$Y_{\text{bus}} = \begin{bmatrix} Y_{11} & Y_{12} & \cdots & Y_{1n} \\ Y_{21} & Y_{22} & \cdots & Y_{2n} \\ \vdots & \vdots & \ddots & \vdots \\ Y_{n1} & Y_{n2} & \cdots & Y_{nn} \end{bmatrix} \tag{3.1}$$

Each element of the Y_{bus} is a complex number and can be expressed in rectangular coordinates as $Y_{ij} = G_{ij} + jB_{ij}$. The admittance matrix is separated into a conductance matrix, G_{bus}, and a susceptance matrix, S_{bus}, in order to avoid having complex numbers in the power flow

equations.

$$Y_{\text{bus}} = G_{\text{bus}} + jB_{\text{bus}} \tag{3.2}$$

Based on Kirchhoff's current law, $\sum I = 0$, the nodal voltage equation can be expressed in matrix form as follows.

$$I = Y_{\text{bus}} \times V \tag{3.3}$$

where I and V are vectors of injected bus current and bus voltage. Each entry of V can be written in terms of magnitude and angle as $|V_j|\angle\delta_{ij}$. Equivalently, each element of Y_{bus} can be expressed as $|Y_{ij}|\angle\theta_{ij}$. Hence for bus i, the ith equation in 3.3 is

$$I_i = \sum_{j=1}^{n} |Y_{ij}||V_j|\angle(\theta_{ij} + \delta_{i,j}) \tag{3.4}$$

The complex power injected at bus i is defined as

$$S_i = P_i + jQ_i = V_i I_i^* \tag{3.5}$$

By combining 3.4 and , and separating into real and imaginary parts, we obtain the power flow equations. Here expressed by voltage in polar coordinates and the admittance in rectangular coordinates.

$$P_i(V, \delta) = V_i \sum_{j=1}^{n} V_j[G_{ij} \cdot \cos(\delta_i - \delta_j) + B_{ij} \cdot \sin(\delta_i - \delta_j)] \tag{3.6}$$

$$Q_i(V, \delta) = V_i \sum_{j=1}^{n} V_j[G_{ij} \cdot \sin(\delta_i - \delta_j) - B_{ij} \cdot \cos(\delta_i - \delta_j)] \tag{3.7}$$

P_i and Q_i are net real and reactive power injections.

The power flow equations, (3.6) and (3.7), represents a set of simultaneous, non-linear and algebraic equations with two unknown variables at each node. They can only be solved using numerical iterative techniques which may converge to the desired solution. The Newton Ralphson (NR) method is one of the most commonly used and has also proven to be the most efficient for larger systems [10].

The unknown values of P_i and Q_i can be found directly from the PF equations, (3.6) and (3.7), hence the problem is to calculate the unknown values of $|V_i|$ and δ_i. The variables, P_i, Q_i, $|V_i|$ and δ_i, can be categorized into a vector of unknown and a vector of specified values. The solution vector, X, contain the unknown voltage magnitudes and angles.

$$X = \begin{bmatrix} \left.\begin{matrix} |V_i| \\ \delta_i \end{matrix}\right\} \text{For each PQ-bus} \\ \\ \left.\begin{matrix} |V_i| \end{matrix}\right\} \text{For each PV-bus} \end{bmatrix} \tag{3.8}$$

The NR method starts with initiating the unknown variables and is using this as a starting point for the iteration. The power flow equations, (3.6) and (3.7), are expanded in Tailor series around the initial estimate resulting in a set of linear equations. In short form, the problem can be written as:

$$\begin{bmatrix} \Delta P \\ \Delta Q \end{bmatrix} = \begin{bmatrix} J \end{bmatrix} \begin{bmatrix} \Delta \delta \\ \Delta |V| \end{bmatrix} \tag{3.9}$$

The left-hand-side matrix is the power mismatch vector, ΔW , it contains the difference between the scheduled and calculated powers. For a P-Q bus both ΔP and ΔQ are included, while for a P-V bus, only ΔP is specified. J denotes the Jacobian matrix and is giving the linearized relationship between small changes in voltage angle and magnitude with small changes in real and reactive power. The right-hand side vector is the solution vector, ΔX containing the unknown voltage magnitudes and angles. The iteration process continues until a convergence criterion is reached, usually that the incremental change power mismatch is at an acceptable value [10].

For large systems, the PF calculations are time-consuming, and the convergence rate is slow. In order to increase the computer time needed, one may decouple the PF equations resulting in constant Jacobi matrices. Consequently, the voltage magnitude is determined mainly by changes in reactive power, whereas voltage angles are sensitive to changes in real power. This can be further simplified by only modeling the active power flow i.e., DC PF. When simplifying the equations, several assumptions regarding the power system are made [26]:

1. Line resistance are negligible i.e. $R \ll X$

2. Voltage angle differences are assumed to be small i.e. $\sin(\theta) = \theta$ and $\cos(\theta) = 1$

3. Magnitudes of bus voltages are set to 1.0 per unit

3.2 Optimal Power Flow

Optimal power flow is a large class of optimization problems and is an important tool in planning, operation, and control of power systems. Generally speaking, a particular objective is achieved while guaranteeing the technical feasibility of the system [28]. In other words, the solution to the OPF problem determines the optimal state of operation. The method seeks to identify the power flow in the network with respect to a defined objective function while meeting all system constraints imposed by electrical laws and limits on control variables. The OPF is a non-linear, non-convex and large-scale optimization problem [4].

The OPF consists of an objective function that we aim to optimize (minimize or maximize), and a set of equality- and inequality constraints. The quality of the proposed solution is highly dependent on the accuracy of the model studied, respectively creating a proper problem description with clearly stated objectives is of great importance. As seen in [29], one way of mathematically express the problem in a general manner is by minimizing an objective subject to operational and physical constraints

$$\begin{aligned} \min \quad & f(\boldsymbol{x}, \boldsymbol{u}, \boldsymbol{y}) \\ \text{s.t.} \quad & g(\boldsymbol{x}, \boldsymbol{u}, \boldsymbol{y}) = 0 \\ & h(\boldsymbol{x}, \boldsymbol{u}, \boldsymbol{y}) \leq 0 \end{aligned} \tag{3.10}$$

where $\boldsymbol{x}$, $\boldsymbol{u}$ and $\boldsymbol{y}$ are the vectors of state- and control variables and parameter values. The objective function, $f(\boldsymbol{x}, \boldsymbol{u}, \boldsymbol{y})$, is a scalar function and represent the goal of the optimization, which could be to minimize the total generation cost or minimize total network losses and so on. $g(\boldsymbol{x}, \boldsymbol{u}, \boldsymbol{y})$ and $h(\boldsymbol{x}, \boldsymbol{u}, \boldsymbol{y})$ are vector functions representing the equality- and inequality constraints respectively.

3.2.1 Variables

Some of the variables that are fixed in conventional power flow analysis are in OPF allowed to vary within their given boundaries so that the objective function is optimized. The variables can

be classified as follows:

- **Control variables:** are controllable and can be actively used to alter the power flow in order to optimize the objective function and meet the constraints. Control variables may include active and reactive power generation of all buses except the slack bus, voltage of PV-buses and tap settings of transformers, etc.
- **State variables:** includes all variables that can describe a unique state of the power system and describe the response of a system to changes in control variables. Voltage magnitudes, voltage angles, and powers that are not defined as control variables or parameter values are state variables.
- **Parameter values:** represent constant values. Typical parameter values are voltage angle at the slack bus and other given values as active- and reactive power at load buses.

3.2.2 Constraints

The constraints introduce the feasible region of the optimization problem and can be classified into equality- and inequality constraints. Inequality constraints represent the operational limits of the system. Inequality constraints that are usual to include in a power system model are listed below:

Inequality constraints

- **Active power constraint:** The active power generation at a bus cannot be negative and cannot exceed the active generation capacity.
- **Reactive power constraint:** The reactive power generation at a bus cannot be lower than the minimum reactive power capability and cannot exceed the reactive generation capacity at the bus.
- **Voltage constraints:** The voltage magnitude and angles at each bus must be within specified limits.
- **Branch current limit:** Representing the upper bounds of the line current limit, making sure that the maximal thermal limits of the branches are not exceeded. This may either be expressed by the current magnitude or by the complex power flow in the branch.

- **Inequality constraints** related to other operational limits such as energy storage or distributed generation.

Equality constraints

The power flow equations, (3.6) and (3.7), form the core of the set of equality constraints in the OPF formulation. These equations imply both a nonlinear formulation and non-convexity in the feasibility region. In order to simplify the representation, one may approximate the equations resulting in a DC PF. The assumptions in the simplification are described in detail in section 3.1. Under normal system operation, the DC model manages to capture the real power transfer quite accurately and has been successfully used in many OPF applications. However, violations like voltage oscillations, transient overvoltages, and system instability are not captured in the DC model. Hence, a full AC PF representation is necessary when evaluating systems under stressed conditions [26].

The characteristics of the distribution network, more specifically the high ratio of R/X and the radial layout, results in variability of voltage across the lines. The phenomena is explained more in detail in section 2.1. When modeling the distribution grid, a full AC OPF is required to capture the voltage variations [4].

3.2.3 Objective Function

The mathematical constraints introduced in the OPF model do not specify one unique network state, but rather a feasibility region. Hence, an enormous number of system states may be computed when only taking the constraints into consideration. The objective function must be included in order to simulate a special, optimal system state [30]. The objective function takes on various forms, some stated below [31]:

- **Minimize total operating cost:** Minimization of the cost for producing electricity is one of the most common objectives in OPF analysis. The mathematical formulation is shown below, minimizing the cost for generating active power.

$$\min_{P_{G,i}} \boldsymbol{c}^\top \boldsymbol{P}_G \tag{3.11}$$

The cost-function can take various forms such as a constant value, quadratic function or

a time-varying function. The three formulations and there influence on the simulation result are studied in the case studies implemented.

- **Maximize social welfare:** When the objective is to maximize social welfare, the mathematical formulation aim to maximize the sum of producer and consumer surplus, or alternatively the sum of the generator costs and the consumer benefits. Thus in comparison to an objective of minimizing generation costs, the maximization of social welfare also includes the end users in the objective.

- **Maintaining a constant voltage profile:** I order to avoid voltage instability problems, the power system operators may want to contain a stable voltage profile across the system nodes. OPF with the objective of a constant voltage profile is particularly relevant in a distribution grid with DG, as the integration of renewable production can introduce more voltage variations (see sec. 2.1).

3.3 Multi-Period Optimal Power Flow

Conventionally OPF methods optimize the operation of a power system for a snapshot in time and are unable to model time-related constraints. The inclusion of flexible resources in the power system requires a simultaneous solution of time-coupled OPF problems, referred to as multi-period or dynamic OPF problems. When including storage in the system, we are allowing energy to be stored at one point in time and dispatching it at different times. Hence, decisions of charging/discharging in one period affects the optimal decisions taken in other periods. Thus the problem takes on a multistage character [4, 32].

A general formulation of a multi-period AC OPF is presented in [33]. The model consists of an objective function spanning a future time horizon and equality- and inequality constraints.

$$\begin{aligned} \min \quad & F(X) \\ \text{s.t.} \quad & G(X) = 0 \\ & H(X) \leq 0 \end{aligned} \tag{3.12}$$

In a standard AC OPF problem the power system consists of n_b buses, n_g generators, n_l lines and n_s storage units. When extending to a multi-period problem, the time horizon is divided

into T time periods [34]. This results in a system with $T \cdot n_b$ buses, $T \cdot n_g$ generators, $T \cdot n_l$ lines and $T \cdot n_s$ storage units. When mathematically formulating a multi-period OPF, each time period also requires a single copy of all variables. Hence the variables are duplicated into T time series. And consequently, the optimization vector, X, is a column vector with the number of rows equal to the sum of state and control variables times number of time-periods. Thus, the optimization vector becomes

$$X = [x_1 \;\; x_2 \;\; \dots \;\; x_t \;\; \dots \;\; x_T]^\top \tag{3.13}$$

where

$$x_t = [\delta_t \;\; V_t \;\; P_t \;\; Q_t \;\; E_t \;\; P_t^{\mathrm{ESS,c}} \;\; P_t^{\mathrm{ESS,d}}]^\top_{1\times v} \tag{3.14}$$

The network must also obey the typical OPF constraints, such as the power flow equations and limits on system variables, during each time-step independently [32]. Thus these constraints are duplicated for each period. The authors of [33] explained this by the vectors of equality- and inequality constraints, $G(X)$ and $H(X)$, shown below. Both vectors include linear- and non-linear constraints, illustrated by $-$ and $\sim$.

$$G(X) = \begin{bmatrix} \tilde{g}(x_{t=1}) \\ \tilde{g}(x_{t=2}) \\ \vdots \\ \tilde{g}(x_{t=T}) \\ \bar{g}(x_{t=1}) \\ \bar{g}(x_{t=2}) \\ \vdots \\ \bar{g}(x_{t=T}) \end{bmatrix} \qquad H(X) = \begin{bmatrix} \tilde{h}(x_{t=1}) \\ \tilde{h}(x_{t=2}) \\ \vdots \\ \tilde{h}(x_{t=T}) \\ \bar{h}(x_{t=1}) \\ \bar{h}(x_{t=2}) \\ \vdots \\ \bar{h}(x_{t=T}) \end{bmatrix} \tag{3.15}$$

Furthermore, additional variables and constraints are incorporated, describing the inter-temporal characteristics of the flexible resource. Assuming that the flexible resource is battery storage, the energy stored E_t is an example of an inter-temporal variable. The value of E_t depends on previous E_t- and charging/discharging values, which results in an inter-temporal constraint.

One can say that a multi-period OPF is a simultaneous formulation of T OPF problems,

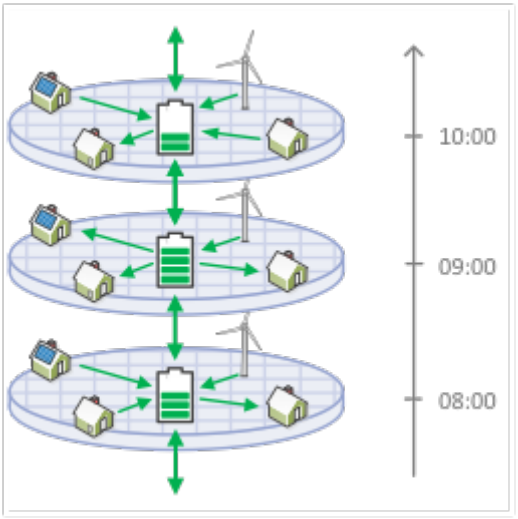

Figure 3.1: Illustrating the idea of a multi-period OPF model [35]

depicted in figure 3.1. Figure 3.1 aims to illustrate the idea of a multi-period optimization model and how the model takes into account the time variations in distributed production, load, and electricity prices. Let's say that we perform a multi-period OPF over a time horizon of 24 hours with time steps $\Delta t = 1$ hour. The figure (3.1) depicts the time-steps from 08:00-10:00 and shows how the amount of energy stores varies between periods. Studying the situation at 08:00, the vertical arrows illustrate how the storage is being charged by arrows pointing towards the battery and discharged by arrows pointing away from the battery. The horizontal arrows illustrate how the amount of energy stored in the battery is dependent on the values of previous time steps and will impact the values in the next time step.

3.4 Optimization Methods

There are many ways to classify the variety within optimization problems: whether they are linear or non-linear, convex or non-convex, dynamic or static, stochastic or deterministic. The multi-period AC OPF problem studied in this thesis is characterized by being non-linear, non-convex, and dynamic, making it challenging to develop algorithms that guarantee the optimal solution. An optimization problem is non-linear if either the objective function or any of the constraints contain non-linear terms. Besides, the problem being non-convex means that there is a possibility of having both local and global optima. The term dynamic refers to the process of optimizing the objective over a period of time.

Numerous of solution methods for solving the AC OPF problems have been proposed in the

literature. The majority of the traditional techniques utilize one of the following algorithms: Newton's method, Simplex method, interior point method, sequential linear programming, and sequential quadratic programming [36]. Some of these methods solve the original non-linear and non-convex problem, while others try to find the solution of a linearized approximation of the problem.

3.4.1 The Interior Point Algorithm of `fmincon`

The multi-period OPF problem in this thesis is implemented using `fmincon`, a built-in optimization solver in MATLAB Optimization Toolbox that can solve constrained, non-linear optimization problems. `fmincon` finds the constrained minimum of a scalar function of several variables given an initial estimate. The user can choose between four different options for the optimization solution algorithm used by the `fmincon` function: interior-point, sequential quadratic programming, active set, and trust region-reflective optimization. Interior point algorithms are broadly applied to solve non-linear optimization problems and especially AC OPF problems [4]. This is also the chosen algorithm in this thesis.

The interior point algorithm of `fmincon` transforms the original problem consisting of both equality and inequality constraints into an approximate problem with only equality constraints and a *barrier function* that "pushes" the decision variables into the feasible region [4]. If the original optimization problem is given by (3.10), then the approximate problem is given by

$$\begin{aligned} \min_{x,s} \quad & f_\mu(x) - \mu \sum_i \ln(s_i) \\ \text{subject to} \quad & h(x) = 0 \\ & g(x) + s = 0 \end{aligned} \tag{3.16}$$

Where s_i are slack variables, there are as many of them as there are inequality constraints in the original problem. The slack variables are restricted to be positive such that $\ln(s_i)$ is defined [37]. The barrier terms are logarithmic and added to the objective for each slack variable. μ is always positive and converging towards zero during the iteration process. As μ is approaching zero, the minimum of the approximate objective, f_μ, should approach the minimum of the original objective function f.

When trying to solve an optimization problem, there are different strategies one may utilize.

The `fmincon` seeks to find the optimum by using a line search method, which generally starts with computing a search direction p_k and then identifies a distance α_k for each iteration [38]. Thus the iteration is given by

$$x_{k+1} = x_k + \alpha_k p_k \tag{3.17}$$

Two search methods are included in the `fmincon` interior point algorithm, namely Newton step and conjugate gradient step. When determining the search direction, the Newton step algorithm is based on the second order derivatives of the objective function while the conjugate gradient method exploits the gradient of the objective function [4]. By default, the algorithm first attempts to take a Newton step [37].

A further, full treatment of the interior point algorithm of `fmincon` is not given here as the thesis is not focusing on the optimization-intensive mathematics. For more information on this technique, the reader might see [38], [39] and [37] for a comprehensive presentation.

Chapter 4

Literature Review

This chapter presents a review of existing research and available literature on multi-period AC OPF. A small survey of papers studying the relevant subject is executed, comparing the different approaches in terms of their methodologies, objective function, and constraints.

4.1 Optimal Power Flow in Literature

Optimal Power Flow is an important technical and economical tool and has an undeniable role in the planning and operation of electric power systems. Ever since Carpentier introduced the OPF in 1962, the work on OPF has drawn a lot of attention [40]. Thus, OPF is a well-researched field of study, and a vast amount of literature discussing the topic has previously been published [4]. The research work is covering a wide range of objectives, decision variables, and constraints, and there is ample of different solution methods available. Technological developments and trends are driving the need for new ways of analyzing the power system. Thus new models and solution methods for the OPF problem is established. In later years, there has been an upsurge of research activity handling OPF in the distribution network. The escalation of interest can be explained by the ongoing transition towards a more flexible and ”smarter” power system. A lot of the developments are integrated at lower voltage levels. The modernization is visible through the growth in the installation of distributed generation and the increasing deployment of flexible resources like energy storage and demand response [4]. This transformation is resulting in a distribution system with a higher level of flexibility and controllability.

The work presented in this thesis is focusing on the formulation of a multi-period AC OPF

when including energy storage in the distribution system. Accordingly, a literature survey is executed on the same topic. Even within this narrow field of study, there has been published a significant amount of work focusing on different aspects of the challenge and adopting various methods and tools for solving the problems. Still, the overall goal of the majority of the work published is to utilize energy storage to facilitate a greater amount of renewable generation in the power system.

4.2 Survey of Multi-Period AC OPF Methods

A literature survey on multi-period AC OPF is completed to elucidate the scope of research done on the relevant subject. Highlights are given in table 4.1. The different approaches are compared in terms of their methodologies, objective function, and constraints. Furthermore, case study networks are reported, and the executive objectives are studied. The work in this thesis is focusing on multi-period OPF with full AC representation of the power flow equations, meaning that AC OPF models for individual time steps are coupled through inter-temporal constraints and the problems are solved without any decomposition of the problem. Only papers introducing models that employ multi-period AC OPF is included in the survey in order to limit the scope.

The reference of the work surveyed is introduced in the first column. Further, the second column briefly states the formulation of the OPF model and the proposed solution method. The modeling language and/or the solver used is also included in the second column if this information is available. The third column gives information about the application of the OPF. In most cases studied, the context of the study is grid-integrated ESS, but there is also one case where EV's are considered. The fourth column presents the test system(s), which the model and solution method is applied. The information given includes the number of buses, and if the system is an IEEE-test system or base on data from a real system. The fifth column states the main objective of the model by introducing the objective function. Further, the modeling of the storage state of charge is presented in column six. The seventh column states which restrictions are included in the papers surveyed.

The authors of [41] aim to minimize system operation costs by determining the optimal combined operation schedule for BESS and wind generation. They formulate both a single-

Reference	OPF model and solution method	Application	Test System	Objective function	Energy storage	Constraints
Optimal Power flow with Energy Storage Systems: Single-period Model vs. Multi-period Model	AC OPF formulated and implemented on two models for comparison: single-period and multi-period. Solved in MATLAB.	Determine optimal combined operation schedule for BESS and wind generation to minimize system operation cost.	IEEE 14-bus and IEEE 57-bus test system over 24 hours.	Minimize total generation cost. Includes both generation cost and battery charging and discharging cost. $Min \sum_{t=1}^{T}\sum_{i=1}^{ng}[c_{0_i} + c_1 P_{G_i}^t + c_2\left(P_{G_i}^t\right)^2] + \sum_{t=1}^{T}\sum_{j=1}^{ns}[c_{d_j}P_{d_j}^t - c_{ch_j}P_{ch_j}^t]$	Energy storage balance equation: $B_i^t = B_i^{t-1} + \left(\eta_{ch_i}P_{ch_i}^t + {P_{d_i}^t}/{\eta_{d_i}}\right)\Delta t$ • Both active and reactive power is modelled • Energy stored at the end of the planning horizon is set to equal to the amount at t=0.	**Equality:** • Power Balance • BESS Energy Balance • BESS Energy continuity – deciding the amount of stored energy at the end of planning horizon **Inequality:** • Voltage magnitude • Active and reactive power generation • Branch current • BESS charging/discharging real power • BESS charging/discharging reactive power • BESS energy capacity • BESS constraint making sure storage is not charged and discharged in the same period
A multi-period Optimal Power Flow Model including Battery Energy Storage	Multi-period AC OPF solved in GAMS.	Study the effect of BESS on power generation scheduling. Minimizing the total cost of operation by deciding the battery charging and discharging schedule to improve peak-shaving effect.	IEEE 30-bus test system over 24 hours. Optimization period is divided into three parts: peak-, valley- and flat hours.	Minimize total generation cost. Considering both cost of generation and charging/discharging cost of BESS. $F = min\sum_{t\in T}\sum_{i\in I}(C_{Gi}^t P_{Gi}^t + C_{BDi}^t - C_{BCi}^t P_{BCi}^t$	Energy storage balance equation: $E_i^t = E_i^{t-1} + \left(P_{BCi}^t \times \eta_{Ci} - \frac{P_{BDi}^t}{\eta_{di}}\right)\times \Delta t$ • Only active power is modelled • Energy stored at the end of the planning horizon is set predefined value.	**Equality:** • Power Balance • BESS Energy Balance • BESS Energy continuity – deciding the amount of stored energy at the end of planning horizon **Inequality:** • Voltage magnitude • Voltage angle • Active power generation • BESS active power constraint • BESS energy capacity

						• BESS constraint making sure storage is not charged and discharged in the same period • Ramp rate for conventional generators
Line Loss Reduction with Distributed Energy Storage Systems	Multi-period AC OPF. Solved using an interior-point algorithm by adopting IPOPT as a solver.	Line-loss reduction under a time-varying load profile by optimizing the storage charging/discharging schedule.	3-bus distribution test system. Studied over a 24-hour horizon divided into two periods: peak and valley	Minimizing line-loss over the total time horizon. $min\ F = \sum_{t\in T}\sum_{i\in I}\left(P_{gi,t} - P_{di,t}\right)$	Energy storage balance equation: $E_{st,t} - \eta_{st,t}P_{st,t}T_0 = E_{st,t+1}$ • Only active power is modelled	**Equality:** • Power Balance • BESS Energy Balance **Inequality:** • Voltage magnitude • Active power generation • Reactive power generation • BESS real power constraint • BESS energy capacity
A Multi-temporal Optimal Power Flow for Managing Storage and Demand flexibility in LV Networks	Multi-period AC OPF solved by interior point method.	Minimizing global system losses by optimizing the operation of energy storage and flexible loads.	Portuguese LV-test system studied over a 24-hour horizon with hourly resolution.	Minimize global losses: $\sum_{t=1}^{24}\left(\sum_{i=1}^{n_g}P_{i,t}^{g} + \sum_{j=1}^{n_s}\frac{P_{j,t}^{inj}}{\varepsilon_j^{inj}} + \sum_{k=1}^{n_f}a_k\left(\Delta P_{k,t}^{down} + \Delta P_{k,t}^{up}\right)\right)$	Energy storage balance equation: $SOC_{t,j} = SOC_{t-1,j} + \varepsilon_j^{ch}\cdot P_{t,j}^{ch} - \frac{P_{t,j}^{inj}}{\varepsilon_j^{inj}}$ • Both active and reactive power is modelled	**Equality:** • Power Balance • BESS Energy Balance **Inequality:** • Voltage magnitude • Voltage angle • Active and reactive power generation • Branch flow limit • BESS active power constraint • BESS reactive power constraint • BESS energy capacity

Integration of PEV and PV in Norway Using Multi-Period ACOPF - Case Study	Multi-period AC OPF	Investigation the impact of large-scale PEV penetration when also considering integration of RES like wind, hydropower and PVs. Studying how an optimal charging schedule is advantageous and can introduce flexibility to the system.	147-bus test system representing a Norwegian distribution system.	Minimize the cost of energy imported from upstream grid $Minimize \sum_{t=1}^{T} \lambda_{spot}(t) \cdot P_G(t)$	Energy storage balance equation: $E_{ST,i}(t) = E_{ST,i}(t-1) + \eta_{chrg,i} P_{Sch,i}(t) \Delta t - \frac{P_{Dch,i}(t) \Delta t}{\eta_{dischg,i}}$ where $SOC_i(t) = \frac{E_{ST,i}(t)}{E_{ST,i}^{\max}}$ • Only active power is modelled	**Equality:** • Power Balance • BESS Energy Balance **Inequality:** • Voltage magnitude • Reactive power generation • Branch flow limit • BESS real power constraint • BESS energy capacity

Figure 4.1: Survey of multi-period AC OPF

period and a multi-period AC OPF model and compare the results. Some concluding remarks worth noticing is how the BESS is operated differently in the two modeling aspects. When performing a single-period optimization, the BESS is only operated based on wind power generation, meaning it is charged when wind generation exceeds load and discharged in the opposite case. When performing a multi-period optimization, the charging/discharging schedule also manages to take into account variations in Locational Marginal Pricing (LMP). Thus, the BESS can help improve the hourly LMP by raising low prices and lowering high prices. Reference [1], perform three case studies where different cost models are introduced. The authors study how these cost models influence the optimal charging/discharging schedule of the BESS with the aim of improving the peak-shaving effect. In [42], the authors intend to illustrate how an optimal charging/discharging schedule for distributed energy storage's can reduce the total system line loss. Three case studies are performed on a simple and illustrating 3-bus system: without storage, with one single storage, and with two storages. The authors of [43] propose a multi-period AC OPF algorithm based on forecasted load and a renewable generation that optimizes the charging/discharging schedule of a BESS. The aim of the study is to illustrate how energy storage located in LV networks can mitigate challenges occurring with a higher integration of renewable generation in distribution grids. They are specifically analyzing over- and under voltage situations. In [33], the optimal charging schedule for EVs in a Norwegian distribution network with high penetration of PV production is presented by implementing a multi-period AC OPF. The authors study different charging scenarios and how the optimal EV strategy can minimize the cost of power imported from the upstream grid, and thus utilize more of the renewable production. They also illustrate how over- and under voltage problems in the radials can be mitigated by taking advantage of the available storage capacity in the distribution grid represented by EVs.

4.2.1 Formulation of the Objective Function

The formulation of objective functions is shortly mentioned in the fifth column of table 4.1. Briefly stated, the objective of the papers studied is a minimization of either costs or losses. In [41], the authors aim to minimize the total generation cost. Included in the objective function is both the cost of operating conventional generators and battery storage. The cost of operating conventional generators is formulated as a quadratic function, while the cost of charging/dis-

charging the storage is represented by a linear function. Likewise, the objective of [1] is to minimize the total cost of generation, including both conventional generators and the cost of charging/discharging. In contrary to the above-mentioned paper, all costs are, in [1], formulated as linear functions. In [33], the authors are studying a distribution grid with only renewable generation. The objective function is formulated as a linear function. And its objective is to minimize the cost of electricity brought from the upstream grid. In both [42] and [43] the objective function aim to minimize losses, but this is formulated differently in the two cases. The authors of [42] intend to demonstrate how the deployment of distributed energy storage can reduce line losses. Thus the objective function is minimizing the difference between active power generation and demand. The authors of [43] are studying the system losses from a different perspective, as the objective function is minimizing losses related to components in the grid.

4.2.2 Formulation of the Energy Storage Balance Equation

The integration of energy storage adds another degree of computational complexity to the optimal power flow problem as additional inter-temporal variables and constraints must be considered. Thus, the optimal operation of a distribution system with energy storage can be formulated as a multi-period AC OPF, which involves determining the optimal charging/discharging schedule of the BESS.

A BESS consists of multiple components, the main one being the battery bank. Others are monitoring- and control systems, power electronics like converters and inverters, and a power conversion system [44]. Thus, it speaks for itself that creating a true mathematical model is complicated. In OPF-studies the characteristics of the battery are commonly described through a simplified model where self-discharge and battery degradation, among others, are neglected [33]. The BESS is often formulated as a linear function describing the state of charge, including limits on SOC and charging/discharging power. SOC is a measure of the amount of charge stored in a battery with respect to the charge that the battery contains when it is fully charged [45]. A common method for estimating this value is called coulomb counting. The technique is based on integrating the active flowing current over time to derive the total sum of energy entering or leaving the battery [46]. The result is a capacity measured in ampere-hours (Ah). In literature, the term SOC is commonly being used for counting watt-hours (Wh), which is not

the same as ampere-hours. The reason is that participants in the electricity market are trading energy, measured in Wh, and not electric charge, measured in Ah. Thus, throughout this study, SOC is used in conjunction with watt-hours. The term stored electrical energy is also used in literature, this quantity is not a fraction of the total capacity, but used to describe the actual amount of energy stored.

In all papers surveyed, the state of charge/energy stored equation is formulated as a discrete-time first order-difference equation with a sampling-time, Δt. In most papers $\Delta t = 1$, and thus some formulations omits Δt. There is one noticeable distinction in the formulation, namely the approach for taking into account whether the storage is being charged or discharged. Some papers solve this problem by splitting the power into two components: $P = P_{\text{charging}} + P_{\text{discharging}}$, while others introduce a binary variable. A more detailed description of the formulation of the energy storage balance equation is given when a multi-period AC OPF model is introduced in chapter 5.

Chapter 5

General Methodology and Modeling in MATLAB

This thesis work aims to provide the reader with a pedagogical introduction to the modeling and implementation of a multi-period AC OPF. With this in mind, the following chapter begins with presenting a simple mathematical model including general assumptions and notations. Thereafter the syntax of the solver used is introduced. None of the work studied in the previous chapter, or literature found by searching the internet, explains how a typical mathematical model is implemented using commercial software. Thus, the minor modifications applied to the model to be in a format suited for the solver is elucidated.

5.1 Optimization Problem Formulation

5.1.1 Assumptions

The following assumptions have been made on the system characteristics to simplify the problem:

1. Power system in steady-state operation and under balanced conditions.

2. Power generation and demand at all buses except at slack bus are assumed to be known.

3. Energy storage is included in the system but does only supply active power.

5.1.2 Notation

Indices:

i, j	Bus indices
t	Time instance

Sets:

T	Time periods
G	Generators
L	Loads

Parameters:

Δt	Time step increment
$S_{i,j}^{\min}, S_{i,j}^{\max}$	Minimum and maximum limit of branch flow from bus i to j
$P_i^{\min}, P_i^{\max}$	Minimum and maximum limit of active power at i^{th} bus
$Q_i^{\min}, Q_i^{\max}$	Minimum and maximum limit of reactive power at i^{th} bus
$V_i^{\min}, V_i^{\max}$	Minimum and maximum limit of voltage magnitude at i^{th} bus
$\delta_i^{\min}, \delta_i^{\max}$	Minimum and maximum limit of voltage angle at i^{th} bus
η_c, η_d	Charging and discharging efficiency of the storage
$E^{\max}$	Rated energy capacity of storage

Variables:

$P_{G,i}(t), Q_{G,i}(t)$	Active and reactive power production at i^{th} bus at time t
$P_{L,i}(t), Q_{L,i}(t)$	Active and reactive power demand at i^{th} bus at time t
$P_{d,i}^{\mathrm{BESS}}(t)$	Active power discharging from the storage at i^{th} bus at time t
$P_{c,i}^{\mathrm{BESS}}(t)$	Active power charging to the storage at i^{th} bus at time t
$E(t)$	Energy stored at time t

5.1.3 Mathematical Model

The multi-period AC OPF model is presented and explained below. The objective function is minimizing the cost of generation over time horizon T while upholding energy balance and physical constraints.

Objective function:

The objective function is minimizing the active generation cost, and the generators are assumed to be modeled by a quadratic function. a_i, b_i and c_i are the cost coefficients. The cost of generating power from renewable sources is assumed to be zero, the same applies to the cost of charging and discharging battery storage.

$$\min \sum_{t=1}^{T} \sum_{i \in G} a_i P_{G,i}^2(t) + b_i P_{G,i}(t) + c_i \tag{5.1}$$

Power balance equations:

The entire AC representation of the power balance equations is included. The equations are stating that both real and reactive power injected at each node must equal the sum of generation and load at that exact node i.e., ensuring power balance at each bus.

$$P_{G,i}(t) - P_{L,i}(t) + P_{d,i}^{\mathrm{BESS}}(t) - P_{c,i}^{\mathrm{BESS}}(t) = P_i(V, \delta) \tag{5.2}$$

$$Q_{G,i}(t) - Q_{L,i}(t) = Q_i(V, \delta) \tag{5.3}$$

$P_i(V, \delta)$ and $Q_i(V, \delta)$ are the active and reactive power flow equations respectively, see (3.6) and (3.7). Note that only the active power contribution from the energy storage is modelled.

Generation constraints:

These constraints make sure that the real and reactive generation does not exceed its operational limitations.

$$P_i^{\min} \leqslant P_i(t) \leqslant P_i^{\max} \tag{5.4}$$

$$Q_i^{\min} \leqslant Q_i(t) \leqslant Q_i^{\max} \tag{5.5}$$

Voltage constraints:

The voltage constraints state that both voltage magnitude and angles must be kept within its range.

$$V_i^{\min} \leqslant V_i(t) \leqslant V_i^{\max} \tag{5.6}$$

$$\delta_i^{\min} \leqslant \delta_i(t) \leqslant \delta_i^{\max} \tag{5.7}$$

Thermal constraints:

The power flow is bounded by the thermal limits of the lines, which can be formulated as the following apparent power limits.

$$S_{i,j}^{\min} \leqslant S_{i,j}(t) \leqslant S_{i,j}^{\max} \tag{5.8}$$

Battery constraints:

In OPF analysis, the modeling of the battery is kept fairly simple. The storage is defined by its energy- and power capacities, charging- and discharging efficiency. The BESS is modeled as generators injecting power to the grid. Charging (c) and discharging (d) are separated into different generators, and it is assumed that the battery only provides active power.

$$P^{\mathrm{BESS}}(t) = P_c^{\mathrm{BESS}}(t) + P_d^{\mathrm{BESS}}(t) \tag{5.9}$$

The following constraint, the energy storage balance equation, represents the energy stored in the battery at the termination of time-step t. In each operating period, the energy stored is either increased or decreased according to (5.10). The equation link successive time-steps, and is describing how the stored energy is dependent on the previously stored energy in the battery and the power charged or discharged during the current time-step.

$$E(t) = E(t-1) + \eta_c P_c^{\mathrm{BESS}} \cdot \Delta t - \frac{P_d^{\mathrm{BESS}}}{\eta_d} \cdot \Delta t \tag{5.10}$$

where η_c and η_d are the associating charging- and discharging efficiency, which is assumed

to be constant throughout the simulation.

Several inequality constraints are also describing the character of the BESS. The following restrictions are constraining the charging or discharging power, specifying at which rate the storage can be charged or discharged.

$$0 \leqslant P_c^{\mathrm{BESS}}(t) \leqslant P_c^{\max} \tag{5.11}$$

$$0 \leqslant P_d^{\mathrm{BESS}}(t) \leqslant P_d^{\max} \tag{5.12}$$

If both $P_c^{\mathrm{BESS}}(t)$ and $P_d^{\mathrm{BESS}}(t)$ are nonzero at the same time, the BESS is being charged and discharged simultaneously. This is an unrealistic solution, and are usually disfavored by the solver. The vector of stored energy in the BESS is bounded to remain between the following limits.

$$0 \leqslant E(t) \leqslant E^{\max} \tag{5.13}$$

5.1.4 Model Formulation

The model formulation, including the objective function as well as equations and constraints, is given as follows:

$$
\begin{aligned}
\min \quad & \sum_{t=1}^{T} \sum_{i \in G} a_i P_{G,i}^2(t) + b_i P_{G,i}(t) + c_i \\
\text{s.t.} \quad & P_{G,i}(t) - P_{L,i}(t) + P_{d,i}^{\mathrm{BESS}}(t) - P_{c,i}^{\mathrm{BESS}}(t) = P_i(V, \delta) \\
& Q_{G,i}(t) - Q_{L,i}(t) = Q_i(V, \delta) \\
& P_i^{\min} \leqslant P_i(t) \leqslant P_i^{\max} \\
& Q_i^{\min} \leqslant Q_i(t) \leqslant Q_i^{\max} \\
& V_i^{\min} \leqslant V_i(t) \leqslant V_i^{\max} \\
& \delta^{\min} \leqslant \delta_i(t) \leqslant \delta^{\max} \\
& S_{i,j}^{\min} \leqslant S_{i,j}(t) \leqslant S_{i,j}^{\max} \\
& P^{\mathrm{BESS}}(t) = P_c^{\mathrm{BESS}}(t) + P_d^{\mathrm{BESS}}(t) \\
& E(t) = E(t-1) + \eta_c P_c^{\mathrm{BESS}} \cdot \Delta t - \frac{P_d^{\mathrm{BESS}}}{\eta_d} \cdot \Delta t \\
& 0 \leqslant P_c^{\mathrm{BESS}}(t) \leqslant P_c^{\max} \\
& 0 \leqslant P_d^{\mathrm{BESS}}(t) \leqslant P_d^{\max} \\
& 0 \leqslant E(t) \leqslant E^{\max}
\end{aligned}
\tag{5.14}
$$

5.2 Modelling in MATLAB

This section explains how the model presented above is implemented using commercial software. The model is written in MATLAB and solved using `fmincon`, which is a built-in optimization solver in MATLAB Optimization Toolbox.The model is written in MATLAB and solved using `fmincon`, which is a built-in optimization solver in MATLAB Optimization Toolbox. All parameter data is read from Excel and loaded to MATLAB. The general formulation of the multi-period AC OPF model, given in (5.14), needs some minor modifications to be in a format suited for the `fmincon` solver [47]. `fmincon` calculate the minimum of a constrained multi-variable function given by the following syntax:

$$\text{[x,fval,exitflag,output,lambda,grad,hessian]} = \text{fmincon(fun,x0,A,b,Aeq,beq,lb,ub,nonlcon,options)} \quad (5.15)$$

Which is mathematically written as:

$$\min f(x) \text{such that} \begin{cases} c(x) \leqslant 0 \\ ceq(x) = 0 \\ A \cdot x \leqslant b \\ Aeq \cdot x = beq \\ lb \leqslant x \leqslant ub \end{cases} \quad (5.16)$$

x, lb, ub, b and beq are vectors, A and Aeq are matrices, $c(x)$ and $ceq(x)$ are functions that return vectors and $f(x)$ is a function that returns a scalar. $f(x)$, $c(x)$, and $ceq(x)$ can be nonlinear functions [47].

The objective function accepts the optimization vector, x, extracts the relevant variables and multiply these with a cost vector, assuming that the objective is to minimize operating costs. Each element of the cost vector corresponds to the value of increasing a decision variable by one unit. The objective function returns a scalar f that is to be minimized by the solver.

The non-linear equality- and inequality constraints are given to the solver as a function, *nonlcon*, accepting the vector of state variables and returning two arrays, $ceq(x)$ and $c(x)$. In the case of a multi-period AC OPF problem, the non-linear equality constraints are the power balance equations at all buses for all time-steps. The non-linear inequality constraints are included if the branch current limit is represented by the thermal capacity of the branches, i.e., limitations in the complex power flowing.

The upper- and lower bounds on variables are specified as real vectors limiting the state variables. The number of elements in lb and ub must equal the number of elements in x.

The mathematical model takes on a multi-period character due to the energy storage balance equation. The equation is a linear equality constraint and must be given as input to the solver on the following form: $Aeq \cdot x = beq$ [47]. Aeq is an $m \times n$-matrix, which represent m equations on a variable x with n components. beq is a vector with m components. When modeling a

multi-period AC OPF, m is equal to the number of periods, and n is the number of time-periods multiplied with the number of state variables. The energy storage balance equation must be reformulated such that all variables are on the left-hand side (LHS) and right-hand side (RHS) consists only of constants. For $t = 1$ the RHS equals the predefined value of E_0, otherwise RHS equals zero. When assuming time-steps of one hour, making $\Delta t = 1$, the equation describing the energy stored in the battery is reordered as follows:

$$E(t) = E(t-1) + \eta_c P_c^{\text{BESS}} \Delta t - \frac{P_d^{\text{BESS}}}{\eta_d} \Delta t \tag{5.17}$$

For $t = 1$:

$$\Rightarrow E(1) - \eta_c P_c^{\text{BESS}} + \frac{P_d^{\text{BESS}}}{\eta_d} = E_0 \tag{5.18}$$

And for all other values of t:

$$\Rightarrow E(t) - E(t-1) - \eta_c P_{ch} + \frac{P_d}{\eta_d} = 0 \tag{5.19}$$

When formulating the constraints as a matrix-equation, x is the optimization vector, as shown in equation (5.20). Further, Aeq is the matrix of LHS-coefficients. Aeq is a sparse matrix in which most of the elements are zero. beq consists of one element equal to the predefined value of E_0 and otherwise zero. The matrix equation is shown for a specific example in section 5.3.

For the `fmincon` solver there are several options available to be set by the user. The options are set by using the *optimoptions* function. Some of the options that may be included by the user are listed below, based on reference [47].

- Chose the optimization algorithm to be something else than the default
- Set iterative display, which is a table of statistics describing the calculations in each iteration of the solver, to show the desired information
- Set the maximum number of function evaluations allowed
- Set the maximum number of iterations allowed
- Set the termination tolerance on x

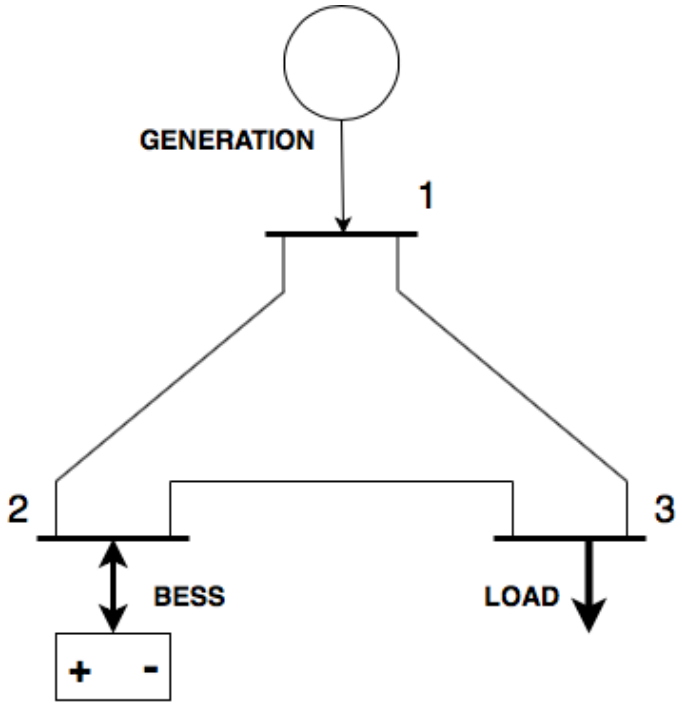

Figure 5.1: Illustration of 3-bus test system

5.3 Illustrative Example

This section presents a small 3-bus test system, the time horizon is divided into 3 steps. The test system is small enough to demonstrate a step-by-step implementation to provide a pedagogical explanation of how to feed a mathematical multi-period AC OPF problem the `fmincon` solver.

5.3.1 3-Bus Test System

The network of the 3-bus test system is depicted in figure 5.1. Bus 1 is the slack bus and is connected to a generator, which represents the main grid. Bus 2 is connected to energy storage. This may charge (draw power) from or discharge (provide power) to the grid. Bus 3 is connected to consumers and represents the demand in the system.

5.3.2 Model

The model introduced in section 5.1.3 is in this section expanded over a time horizon of $T = 3$ and assuming $\Delta t = 1$. For simplicity, the constraint representing thermal limits, equation (5.8), is neglected.

When constructing a multi-period AC OPF over a time horizon T, each period require a copy

of all variables and all constraints are duplicated for the number of periods. This is explained in further detail in section 3.3. For all cases studied in this thesis, the variables of the optimization vector are specified in the following predefined order:

1. Voltage angles of all buses
2. Voltage magnitude of all buses
3. Real power of PV-buses
4. Storage state of charge
5. Reactive power for all buses (except nodes with only storage connected, as they are assumed to only supply active power.)
6. Storage active power charging
7. Storage active power discharging

Thus, for a 3-bus system over a horizon of three time-steps, the optimization vector becomes:

$$\boldsymbol{x} = \begin{bmatrix} \left.\begin{matrix} \delta_1 \\ \delta_2 \\ \delta_3 \\ V_1 \\ V_2 \\ V_3 \\ P_1 \\ E_0^{\mathrm{BESS}} \\ Q_1 \\ Q_2 \\ P_c^{\mathrm{BESS}} \\ P_d^{\mathrm{BESS}} \end{matrix}\right\} \text{For t=1} \\ \left.\begin{matrix} \delta_1 \\ \delta_2 \\ \vdots \\ P_d^{\mathrm{BESS}} \end{matrix}\right\} \text{For t=2} \\ \left.\begin{matrix} \delta_1 \\ \delta_2 \\ \vdots \\ P_d^{\mathrm{BESS}} \end{matrix}\right\} \text{For t=3} \end{bmatrix} \tag{5.20}$$

Objective function:

The extended objective function becomes

$$f = (a_1 P_1^2(1) + b_1 P_1(1) + c_1) + (a_1 P_1^2(2) + b_1 P_1(2) + c_1) \\ + (a_1 P_1^2(3) + b_1 P_1(3) + c_1) \quad (5.21)$$

Power balance equations:

The power balance equations are given by (5.2) and (5.3). In this section, all powers injected or drawn from the node, i.e., (LHS) of the equations, are merged into one variable: net injections, $P_{\text{inj},i}$ and $Q_{\text{inj},i}$. The net injection vectors are defined in terms of the load demand subtracted from the vector of generation. If storage is connected to the node, the active net injection vector is defined as the power charged subtracted from power discharged by the battery. For the three time-steps, we get the following constraints:

First time-step:

BUS 1:

$$Ceq1 = -P_{\text{inj},1}(1) + V_1^2(1)G_{11} + V_1(1)V_2(1)\big[G_{12}\cos(-\delta_2(1)) + B_{12}\sin(-\delta_2(1)\big] + \\ V_1(1)V_3(1)\big[G_{13}\cos(-\delta_3(1)) + B_{13}\sin(-\delta_3(1))\big] \quad (5.22)$$

$$Ceq2 = -Q_{\text{inj},1}(1) - V_1^2(1)B_{11} - V_1(1)V_2(1)\big[B_{12}\cos(-\delta_2(1)) - G_{12}\sin(-\delta_2(1))\big] \\ - V_1(1)V_3(1)\big[B_{13}\cos(-\delta_3(1)) - G_{13}\sin(-\delta_3(1))\big] \quad (5.23)$$

BUS 2:

$$Ceq3 = -P_{\text{inj},2}(1) + V_2^2(1)G_{22} + V_2(1)V_1(1)\big[G_{21}\cos(\delta_2(1)) + B_{21}\sin(\delta_2(1))\big] + \\ V_2(1)V_3(1)\big[G_{23}\cos(\delta_2(1) - \delta_3(1)) + B_{23}\sin(\delta_2(1) - \delta_3(1))\big] \quad (5.24)$$

$$Ceq4 = -Q_{\text{inj},2}(1) - V_2^2(1)B_{22} - V_2(1)V_1(1)\big[B_{21}\cos(\delta_2(1)) - G_{21}\sin(\delta_2(1))\big] \\ - V_2(1)V_1(1)\big[B_{23}\cos(\delta_2(1) - \delta_3(1)) - G_{23}\sin(\delta_2(1) - \delta_3(1))\big] \quad (5.25)$$

BUS 3:

$$Ceq5 = -P_{\text{inj},3}(1) + V_3^2(1)G_{33} + V_3(1)V_1(1)\big[G_{31}\cos(\delta_3(1)) + B_{31}\sin(\delta_3(1))\big] \\ + V_3(1)V_2(1)\big[G_{32}\cos(\delta_3(1) - \delta_2(1)) + B_{32}\sin(\delta_3(1) - \delta_2(1))\big] \quad (5.26)$$

$$Ceq6 = -P_{\text{inj},3}(1) - V_3^2(1) - V_3(1)V_1(1)\big[B_{31}\cos(\delta_3(1) - G_{31}\sin(\delta_3(1))\big] \\ - V_3(1)V_2(1)\big[B_{32}\cos(\delta_3(1) - \delta_2(1)) - G_{32}\sin(\delta_3(1) - \delta_2(1))\big] \quad (5.27)$$

Second time-step:

BUS 1:

$$Ceq7 = -P_{\text{inj},1}(2) + V_1^2(2)G_{11} + V_1(2)V_2(2)\big[G_{12}\cos(-\delta_2(2)) + B_{12}\sin(-\delta_2(2)\big] + \\ V_1(2)V_3(2)\big[G_{13}\cos(-\delta_3(2)) + B_{13}\sin(-\delta_3(2))\big] \quad (5.28)$$

$$Ceq8 = -Q_{\text{inj},1}(2) - V_1^2(2)B_{11} - V_1(1)V_2(2)\big[B_{12}\cos(-\delta_2(2)) - G_{12}\sin(-\delta_2(2))\big] \\ - V_1(2)V_3(2)\big[B_{13}\cos(-\delta_3(2)) - G_{13}\sin(-\delta_3(2))\big] \quad (5.29)$$

BUS 2:

$$Ceq9 = -P_{\text{inj},2}(2) + V_2^2(2)G_{22} + V_2(2)V_1(2)\big[G_{21}\cos(\delta_2(2)) + B_{21}\sin(\delta_2(2))\big] + \\ V_2(2)V_3(2)\big[G_{23}\cos(\delta_2(2) - \delta_3(2)) + B_{23}\sin(\delta_2(2) - \delta_3(2))\big] \quad (5.30)$$

$$Ceq10 = -Q_{\text{inj},2}(2) - V_2^2(2)B_{22} - V_2(2)V_1(2)\big[B_{21}\cos(\delta_2(2)) - G_{21}\sin(\delta_2(2))\big] \\ - V_2(2)V_1(2)\big[B_{23}\cos(\delta_2(2) - \delta_3(2)) - G_{23}\sin(\delta_2(2) - \delta_3(2))\big] \quad (5.31)$$

BUS 3:

$$Ceq11 = -P_{\text{inj},3}(2) + V_3^2(2)G_{33} + V_3(2)V_1(3)\big[G_{31}\cos(\delta_3(2)) + B_{31}\sin(\delta_3(2))\big] \\ + V_3(2)V_2(2)\big[G_{32}\cos(\delta_3(2) - \delta_2(2)) + B_{32}\sin(\delta_3(2) - \delta_2(2))\big] \quad (5.32)$$

$$Ceq12 = -Q_{\text{inj},3}(2) - V_3^2(2) - V_3(2)V_1(2)\big[B_{31}\cos(\delta_3(2) - G_{31}\sin(\delta_3(2))\big] \\ - V_3(2)V_2(2)\big[B_{32}\cos(\delta_3(2) - \delta_2(2)) - G_{32}\sin(\delta_3(2) - \delta_2(2))\big] \quad (5.33)$$

Third time-step:

BUS 1

$$Ceq13 = -P_{\text{inj},1}(3) + V_1^2(3)G_{11} + V_1(3)V_2(3)\big[G_{12}\cos(-\delta_2(3)) + B_{12}\sin(-\delta_2(3)\big] + \\ V_1(3)V_3(3)\big[G_{13}\cos(-\delta_3(3)) + B_{13}\sin(-\delta_3(3))\big] \quad (5.34)$$

$$Ceq14 = -Q_{\text{inj},1}(3) - V_1^2(3)B_{11} - V_1(3)V_2(3)\big[B_{12}\cos(-\delta_2(3)) - G_{12}\sin(-\delta_2(3))\big] \\ - V_1(3)V_3(3)\big[B_{13}\cos(-\delta_3(3)) - G_{13}\sin(-\delta_3(3))\big] \quad (5.35)$$

BUS 2:

$$Ceq15 = -P_{\text{inj},2}(3) + V_2^2(3)G_{22} + V_2(3)V_1(3)\big[G_{21}\cos(\delta_2(3)) + B_{21}\sin(\delta_2(3))\big] + \\ V_2(3)V_3(3)\big[G_{23}\cos(\delta_2(1) - \delta_3(1)) + B_{23}\sin(\delta_2(1) - \delta_3(1))\big] \quad (5.36)$$

$$Ceq16 = -Q_{\text{inj},2}(3) - V_2^2(3)B_{22} - V_2(3)V_1(3)\big[B_{21}\cos(\delta_2(3)) - G_{21}\sin(\delta_2(3))\big] \\ - V_2(3)V_1(3)\big[B_{23}\cos(\delta_2(3) - \delta_3(3)) - G_{23}\sin(\delta_2(3) - \delta_3(3))\big] \quad (5.37)$$

BUS 3:

$$Ceq17 = -P_{\text{inj},3}(3) + V_3^2(3)G_{33} + V_3(3)V_1(3)\big[G_{31}\cos(\delta_3(3)) + B_{31}\sin(\delta_3(3))\big] \\ + V_3(3)V_2(3)\big[G_{32}\cos(\delta_3(2) - \delta_2(2)) + B_{32}\sin(\delta_3(3) - \delta_2(3))\big] \quad (5.38)$$

$$Ceq18 = -Q_{\text{inj},3}(3) + -V_3^2(3) - V_3(3)V_1(3)\big[B_{31}\cos(\delta_3(3) - G_{31}\sin(\delta_3(3))\big] \\ - V_3(3)V_2(3)\big[B_{32}\cos(\delta_3(3) - \delta_2(3)) - G_{32}\sin(\delta_3(3) - \delta_2(3))\big] \quad (5.39)$$

Consequently, $ceq(x)$ is an array consisting of 1 row and columns equal to the number of (buses $\times$ time-steps $\times$ 2). The vector handed to the solver for a 3-bus system optimized over a time horizon of three time-steps then becomes:

$$Ceq = [Ceq1 \;\; Ceq2 \;\; Ceq3 \;\; \ldots \;\; Ceq18]^\top \quad (5.40)$$

Upper and lower bound on variables:

$$V_1^{\min} \leqslant |V_1(1)| \leqslant V_1^{\max} \\ V_1^{\min} \leqslant |V_1(2)| \leqslant V_1^{\max} \quad (5.41) \\ V_1^{\min} \leqslant |V_1(3)| \leqslant V_1^{\max}$$

$$V_2^{\min} \leqslant |V_2(1)| \leqslant V_2^{\max} \\ V_2^{\min} \leqslant |V_2(2)| \leqslant V_2^{\max} \quad (5.42) \\ V_2^{\min} \leqslant |V_2(3)| \leqslant V_2^{\max}$$

$$V_3^{\min} \leqslant |V_3(1)| \leqslant V_3^{\max} \\ V_3^{\min} \leqslant |V_3(2)| \leqslant V_3^{\max} \quad (5.43) \\ V_3^{\min} \leqslant |V_3(3)| \leqslant V_3^{\max}$$

$$\begin{aligned} 0 \leqslant \delta_1(1) \leqslant \pi \\ 0 \leqslant \delta_1(2) \leqslant \pi \\ 0 \leqslant \delta_1(3) \leqslant \pi \end{aligned} \tag{5.44}$$

$$\begin{aligned} 0 \leqslant \delta_2(1) \leqslant \pi \\ 0 \leqslant \delta_2(2) \leqslant \pi \\ 0 \leqslant \delta_2(3) \leqslant \pi \end{aligned} \tag{5.45}$$

$$\begin{aligned} 0 \leqslant \delta_3(1) \leqslant \pi \\ 0 \leqslant \delta_3(2) \leqslant \pi \\ 0 \leqslant \delta_3(3) \leqslant \pi \end{aligned} \tag{5.46}$$

$$\begin{aligned} P_1^{\min} \leqslant P_1(1) \leqslant P_1^{\max} \\ P_1^{\min} \leqslant P_1(2) \leqslant P_1^{\max} \\ P_1^{\min} \leqslant P_1(3) \leqslant P_1^{\max} \end{aligned} \tag{5.47}$$

$$\begin{aligned} E^{\min} \leqslant E(1) \leqslant E^{\max} \\ E^{\min} \leqslant E(2) \leqslant E^{\max} \\ E^{\min} \leqslant E(3) \leqslant E^{\max} \end{aligned} \tag{5.48}$$

$$\begin{aligned} Q_1^{\min} \leqslant Q_1(1) \leqslant Q_1^{\max} \\ Q_1^{\min} \leqslant Q_1(2) \leqslant Q_1^{\max} \\ Q_1^{\min} \leqslant Q_1(3) \leqslant Q_1^{\max} \end{aligned} \tag{5.49}$$

$$\begin{aligned} Q_2^{\min} \leqslant Q_2(1) \leqslant Q_2^{\max} \\ Q_2^{\min} \leqslant Q_2(2) \leqslant Q_2^{\max} \\ Q_2^{\min} \leqslant Q_2(3) \leqslant Q_2^{\max} \end{aligned} \tag{5.50}$$

$$\begin{aligned} 0 \leqslant P_c^{BESS}(1) \leqslant P_c^{\max} \\ 0 \leqslant P_c^{BESS}(2) \leqslant P_c^{\max} \\ 0 \leqslant P_c^{BESS}(3) \leqslant P_c^{\max} \end{aligned} \tag{5.51}$$

$$
\begin{aligned}
0 \leqslant P_d^{BESS}(1) \leqslant P_d^{\max} \\
0 \leqslant P_d^{BESS}(2) \leqslant P_d^{\max} \\
0 \leqslant P_d^{BESS}(3) \leqslant P_d^{\max}
\end{aligned}
\tag{5.52}
$$

The upper and lower bounds are handed to the solver as two vectors, one with the values representing upper bounds and the other representing lower bounds. The values are specified in the same order as the variables of the optimization vector shown in equation (5.20).

Energy storage balance constraint:

$$
\begin{aligned}
E(1) &= E(0) + \eta_c P_c^{\mathrm{BESS}} \Delta t - \frac{P_d^{\mathrm{BESS}}}{\eta_d} \Delta t \\
E(2) &= E(1) + \eta_c P_c^{\mathrm{BESS}} \Delta t - \frac{P_d^{\mathrm{BESS}}}{\eta_d} \Delta t \\
E(3) &= E(2) + \eta_c P_c^{\mathrm{BESS}} \Delta t - \frac{P_d^{\mathrm{BESS}}}{\eta_d} \Delta t
\end{aligned}
\tag{5.53}
$$

The energy storage balance equation is formulated as a matrix equation before given as input to the solver. For the 3-bus system shown here the matrices, Aeq, x and beq, are of the following size $36 \times 3, 1 \times 36$ and 1×3, respectively. A full representation of the matrices is given below. The dots inserted in the Aeq-matrix represent zeros, added due to the limited amount of space on one page. The numbers in the upper row of the Aeq-matrix represent the column-number.

(5.54)

$$
\begin{bmatrix}
\delta_1(1) \\ \delta_2(1) \\ \delta_3(1) \\ V_1(1) \\ V_2(1) \\ V_3(1) \\ P_1(1) \\ E(0) \\ Q_1(1) \\ Q_2(1) \\ P_c(1) \\ P_d(1) \\ \vdots \\ E(1) \\ Q_1(2) \\ Q_2(2) \\ P_c(2) \\ P_d(2) \\ \vdots \\ E(2) \\ Q_1(3) \\ Q_2(3) \\ P_c(3) \\ P_d(3)
\end{bmatrix}
=
\begin{bmatrix}
SOC(0) \\ 0 \\ 0
\end{bmatrix}
\cdot
\begin{bmatrix}
 & & & & & & & & & & & & & & & & & & & & & & & & \\
\cdots & 0 & 1 & 0 & 0 & -\eta_c & \frac{1}{\eta_d} & 0 & \cdots & 0 & 0 & 0 & 0 & \cdots & 0 & 0 & 0 & -\eta_c & \frac{1}{\eta_d} & 0 & \cdots & 0 & 0 & 0 & 0 \\
\cdots & 0 & -1 & 0 & 0 & 0 & 0 & 0 & \cdots & 0 & 0 & 0 & 0 & \cdots & 0 & 0 & 0 & 0 & 0 & 0 & \cdots & 0 & 0 & 0 & 0 \\
\cdots & 0 & 0 & 0 & 0 & 0 & 0 & 0 & \cdots & 0 & 1 & 0 & 0 & \cdots & 0 & 0 & 0 & 0 & 0 & 0 & \cdots & 0 & 0 & 0 & 0
\end{bmatrix}
$$

Chapter 6

Cases and Implementation

This chapter present information regarding the test systems studied in the thesis. The results from the case studies are given in chapter 7. The code for the 3-bus test system is given in appendix B. The system information is formulated in standard MATPOWER format and extracted from an excel-sheet. A qualitative description of the computational procedure is described in the last section of the chapter.

Throughout the rest of this work, the plots are offset to start at zero. The value of input parameters is given at a discrete points in time, and assumed to be constant between two time-steps. This works well for load and generation. It is less intuitive for the stored energy, as it cannot change instantly. Nevertheless, this is how it is shown in the 3-bus case. In the 9-bus case, it is illustrated as a constant value, even though information is given at discrete points in time.

6.1 3-Bus Test System

This section introduces the line characteristics, generation, and energy consumption of the 3-bus test illustrated in figure 5.1. The test system consists of one generator connected to bus 1, a BESS connected to bus 2 and a load at bus 3. The results from applying the multi-period AC OPF model from section 5.1.4 to the test system is given in section 7.1.

The objective function is minimizing the cost of generation from the conventional generator at bus 1, the cost of charging/discharging the battery is assumed to be zero. The load pattern is assumed to be deterministic over the time horizon T and illustrated in figure 6.1. The storage

is assumed to only contribute to active power. Other parameters related to the storage is the storage capacity $E^{\max} = 200MW$, the power capacity $P_c^{\max} = -P_d^{\max} = 50MW$ and the charging- and discharging efficiency $\eta_c = \eta_d = 0.85$. Base values are sat to $100MVA$ and $115kV$. The remaining input parameters are given in tables 6.1 and 6.2 based on [48].

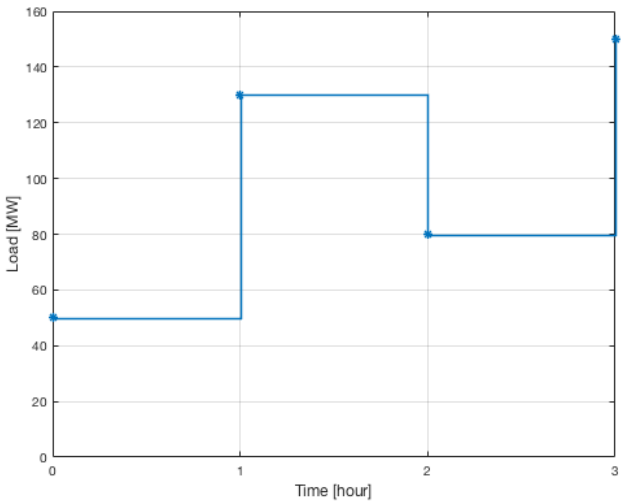

Figure 6.1: Total system load hour by hour

Bus	Vmax	Vmin	Pmax	Pmin	Qmax	Qmin
1	1.0	1.0	200	−200	100	−100
2	1.1	0.9	50	−50	0	0
3	1.1	0.9	–	–	–	–

Table 6.1: Bus data for 3-bus test system

From bus	To bus	R (p.u.)	X (p.u.)
1	2	0.08	0.24
1	3	0.02	0.06
2	3	0.06	0.018

Table 6.2: Line data for 3-bus test system

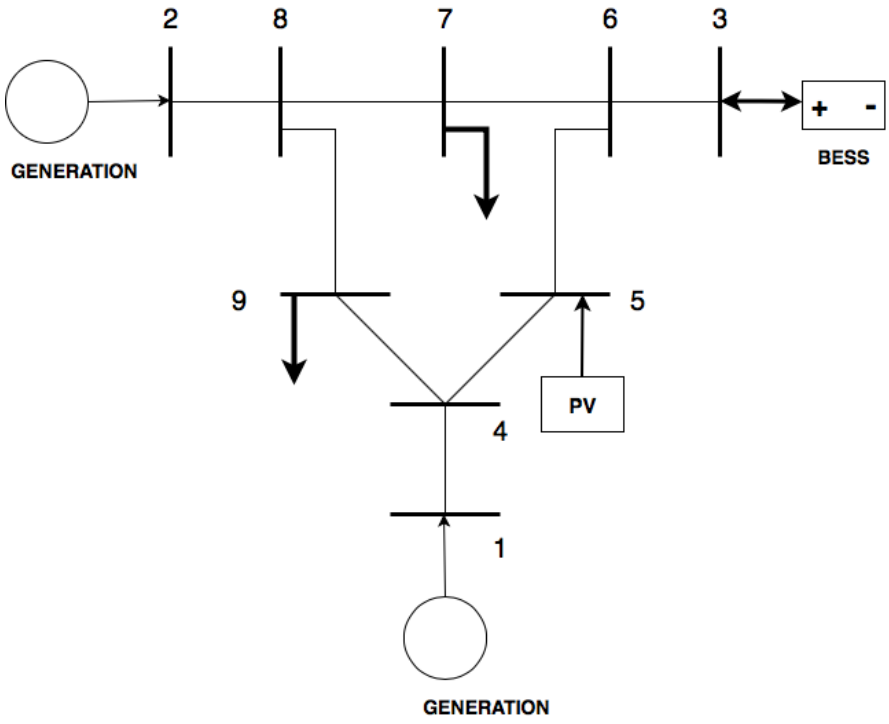

Figure 6.2: Modified IEEE 9-bus system

6.2 Modified IEEE 9-Bus System

In this section, a modified version of the standard IEEE 9-bus system is introduced. The data is readily found by searching the internet, for example, in [49]. The author is fully aware that this system does not represent the expected characteristics of a distribution network. Neither does the system parameters match the typical values, nor is the system of a radial structure. Nevertheless, the study is included to illustrate that the multi-period AC OPF structure presented can be successful in producing the optimal operation strategy of energy storage. Besides, the simplicity of the test case makes it possible to provide the reader with a conceptual understanding of this state-of-art work from the perspective of pedagogical clarity.

The network of the 9-bus test system is depicted schematically in figure 6.2, and the provided information includes grid design, line characteristics, generation, and energy consumption. The model consists of two conventional generators, located at bus 1 and 2. Bus 1 is the slack bus of the system. The test system is assumed to be connected to the external grid through a Point of Common Coupling (PCC), here modeled as a generator connected to bus 1. This results in power only being imported through this point, and not exported. There are two loads present in the system connected to bus 7 and 9. They are representing typical household loads

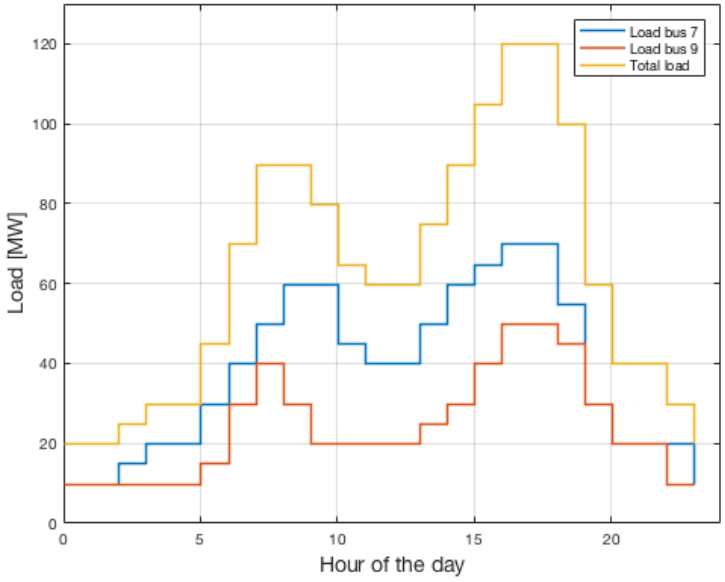

Figure 6.3: Total system load hour by hour

with two peak periods during the day, one in the morning and one in the afternoon. The load pattern is assumed to be deterministic over the time horizon, T, and illustrated in figure 6.3.

The energy storage is connected to bus 3, this may discharge (or charge) power to (from) the grid. Note that we assume that the BESS does not provide reactive power support to the grid, hence only the active power of the battery is modelled. Other parameters related to the storage is the storage capacity $E^{\max} = 200MW$, the power capacity $P_c^{\max} = -P_d^{\max} = 50MW$ and the charging- and discharging efficiency $\eta_c = \eta_d = 0.85$.

Distributed generation is connected to bus 5, and included in the system as a PV plant. The power produced from the PV plant is assumed to be deterministic over the optimization horizon, T, and shown in figure 6.4. Production from the PV plant is given to the model as input that is varying throughout the optimization horizon. Since it is a known value, it is modeled as a negative load injecting power to the grid.

The objective function is minimizing the cost of generation from conventional generators i.e., minimizing the cost of operating the generators connected to buses 1 and 2. It is formulated as a quadratic function, which is explained more in detail in section 5.1.3. The values of the cost coefficients are kept as the original values in the IEEE 9-bus test system.

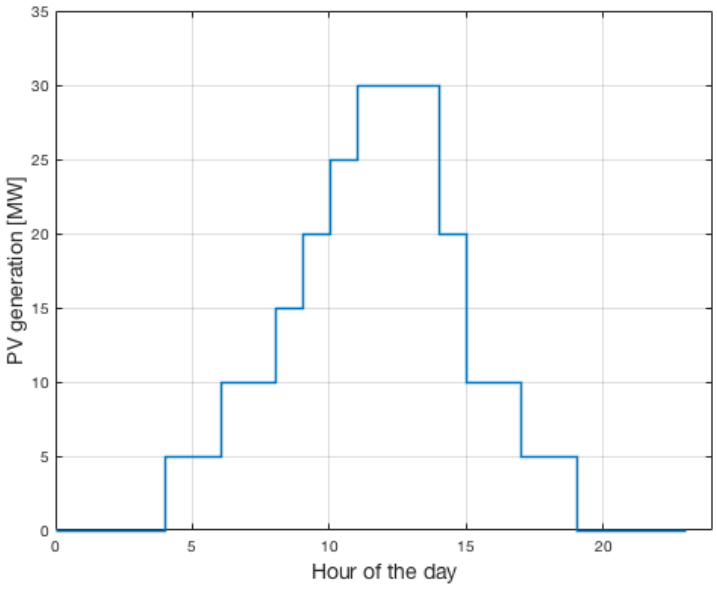

Figure 6.4: PV generation hour by hour

Table 6.3 present the maximum and minimum constraints on bus voltage, as well as bounds on active power and reactive power. Some modifications from the standard system are depleted, as PV generation, and battery storage are included in the test grid. In table 6.4, the network line data is shown, this is equivalent to the standard test system. The base values of the system are $100MVA$ and $115kV$. The problem is run for a time horizon of $T = 24$h with hourly resolution, i.e. $\Delta t = 1$h. The model is optimized across all slots simultaneously to handle charging and discharging across multiple time-steps.

Bus	Vmax [p.u.]	Vmin [p.u.]	Pmax [MW]	Pmin [MW]	Qmax [MW]	Qmin [MW]
1	1.0	1.0	200	−200	100	−100
2	1.1	0.9	50	−50	50	−50
3	1.1	0.9	50	0	0	0
4	1.1	0.9	-	-	-	-
5	1.1	0.9	50	0	0	0
6	1.1	0.9	-	-	-	-
7	1.1	0.9	-	-	-	-
8	1.1	0.9	-	-	-	-
9	1.1	0.9	-	-	-	-

Table 6.3: Bus data for IEEE 9-bus test system

From bus	To bus	R [p.u.]	X [p.u.]	B [p.u.]
1	4	0	0.0576	0
4	5	0.0170	0.0920	0.158
5	6	0.0390	0.1700	0.358
3	6	0	0.0586	0
6	7	0.0119	0.1008	0.209
7	8	0.0085	0.0720	0.149
8	2	0	0.0625	0
8	9	0.0320	0.1610	0.306
9	4	0.0100	0.0850	0.176

Table 6.4: Line data for IEEE 9-bus test system

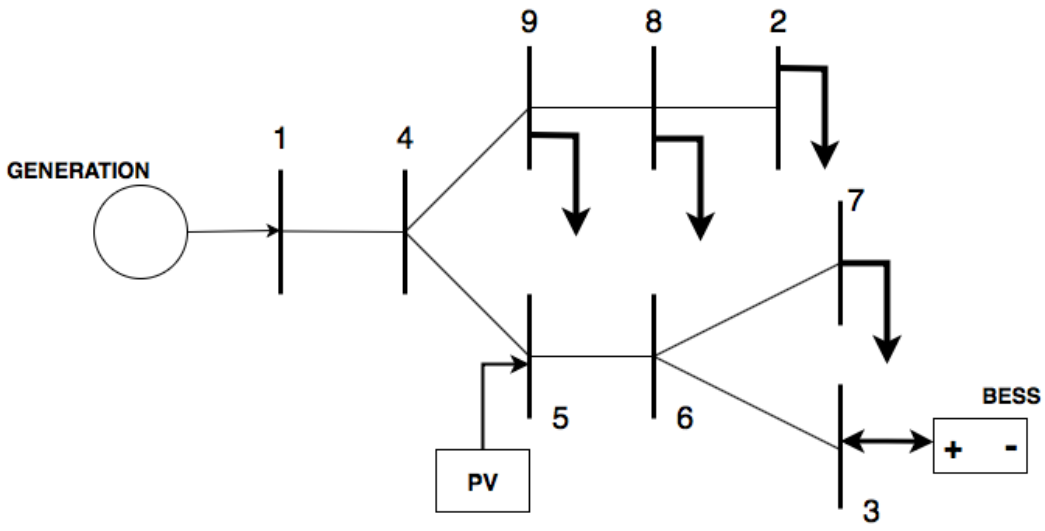

Figure 6.5: Radial 9-bus test system

6.3 Radial 9-Bus System

In this section, a test system based on the 9-bus IEEE system in the section above introduced. The system is modified such that the structure and value of parameters are more like a typical distribution system. In the two above mentioned test-systems, some system values have been exaggerated to illustrate the characteristics of the system operation more clearly. This study is included to get more realistic results.

The network of the 9-bus system is depicted schematically in figure 6.5, it is visible that the structure is almost identical with the 9-bus introduced in the above section. The author has made some structural changes as follows: the branch between nodes 7 and 8 is removed, the generator at bus 2 is replaced by a load, and a load is added at bus 8. The information regarding load and generation are based on values from [33], where the authors are investigating a residential area in Norway. Information regarding bounds on bus voltage and power generation are given in table 6.5.

Further are load pattern and PV production during the optimization horizon depicted i figure 6.6 and 6.7, respectively. The line data is as given in 6.4. The energy storage is located at bus 3, the values of maximum storage capacity and charging/discharging efficiencies are chosen to correspond to values given for a Tesla Powerpack [50]. Accordingly, the maximum storage capacity is 210 kWh, the power capacity $P_c^{\max} = -P_d^{\max} = 50\text{kW}$ and the charging- and discharging efficiency where set to $\eta_\text{c} = \eta_\text{d} = 0.94$.

Bus	Vmax [p.u.]	Vmin [p.u.]	Pmax [MW]	Pmin [MW]	Qmax [MW]	Qmin [MW]
1	1.0	1.0	200	−200	100	−100
2	1.1	0.9	–	–	–	–
3	1.1	0.9	0.0005	0	0	0
4	1.1	0.9	-	-	-	-
5	1.1	0.9	0.0003	0	0	0
6	1.1	0.9	-	-	-	-
7	1.1	0.9	-	-	-	-
8	1.1	0.9	-	-	-	-
9	1.1	0.9	-	-	-	-

Table 6.5: Bus data for radial 9-bus test system

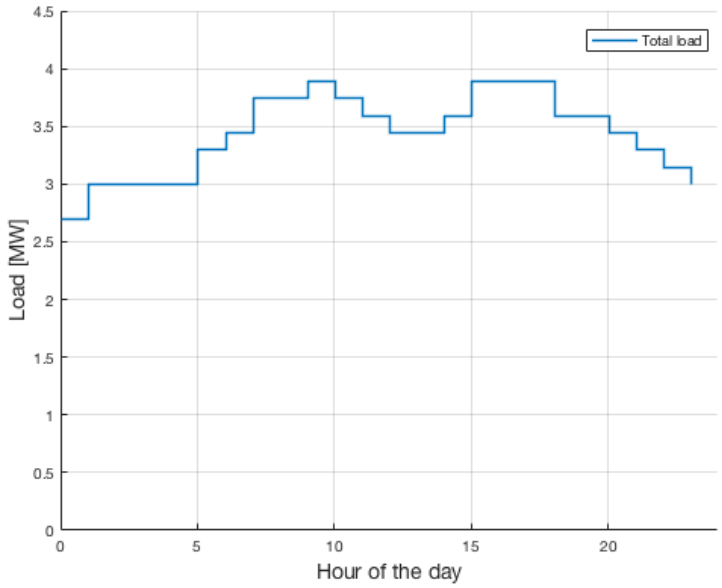

Figure 6.6: Total system load hour by hour

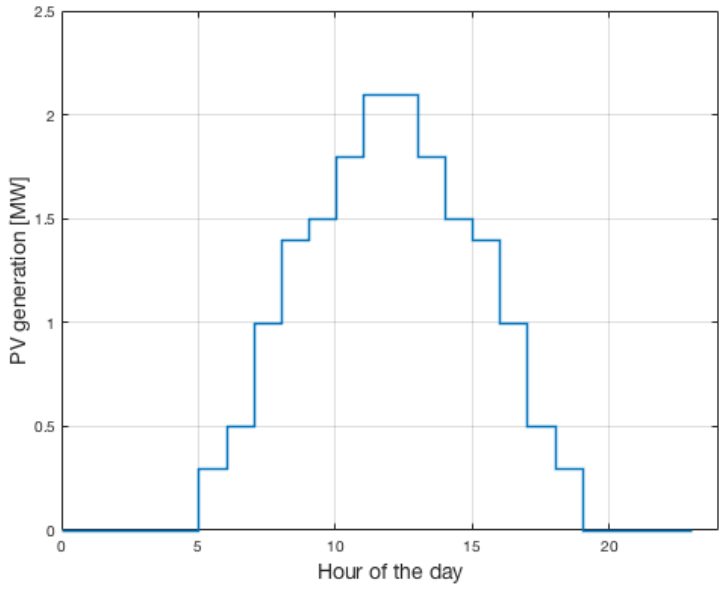

Figure 6.7: PV generation hour by hour

6.4 Implementation

A qualitative description of the computational procedure is presented below. A simple flow chart showing the main steps are also included in fig. 6.8.

1. Load power system data from specified excel files. The information required is generation data, load data for each time step and branch data, including flow limits and generation cost.

2. Use loaded system data and defined base values to construct vectors of specified values such as generation, $P_{G,i}$ and $Q_{G,i}$ and load, $P_{L,i}$ and $Q_{L,i}$. Make sure all vectors contain values in p.u.

3. Create vectors of upper- and lower bounds on state variables.

4. Chose an initial starting point.

   The choice of initial starting point is important in nonlinear optimization and hence also in AC OPF. There are commonly two approaches to adopt: flat or warm start. In a flat start procedure the voltage magnitudes are set to 1.0 p.u. and voltage angles to zero. When using a warm start, a pre-solved load flow is used as initial values for voltage magnitude and angles [30].

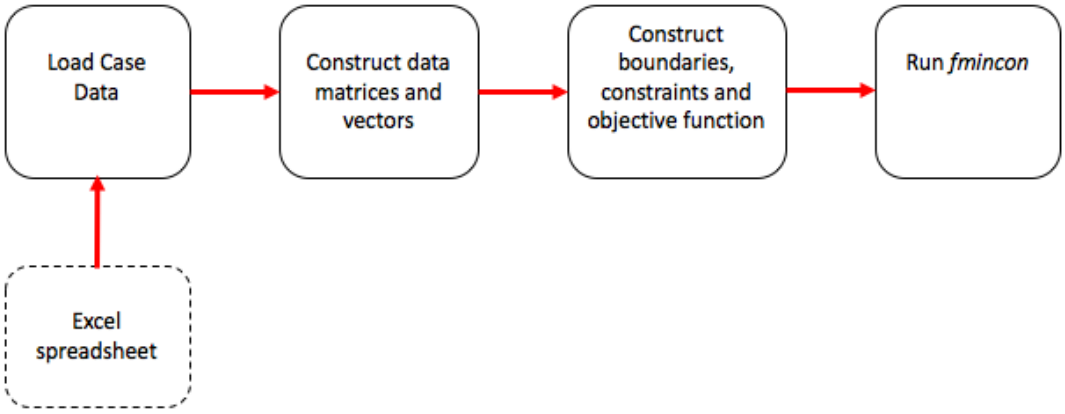

Figure 6.8: AC OPF architectural flowchart

5. Expand vectors of upper- and lower bounds and the initial guess for all periods.

6. Define linear constraints i.e., the state of charge battery equation. This is formulated as a matrix-equation, and the construction is explained more in detail in section 5.2.

7. Define non-linear constraints i.e. power flow equations and flow limits (if included as complex power).

8. Specify options.

9. Run optimization by calling `fmincon`.

6.4.1 Implementation of Non-Linear Constraints

As previously mentioned, and also clarified through the illustrative 3-bus example, when expanding an AC OPF model over a time horizon, the complexity of the problem escalates. Even for a 3-bus network over a time horizon of three intervals, the problem gets way more complicated to solve than a single-period AC OPF. Some of the more time-consuming calculations are to determine the non-linear constraints, i.e., the power balance equations and the restrictions on power flow. To ease this process, one may exploit how these constraints are handled in MATPOWER [1].

From the MATPOWER User Manual, [52], the AC power balance equation is expressed as:

[1]" MATPOWER is a package of free, open-source Matlab-language M-files for solving steady-state power system simulation and optimization problems. It is intended as a simulation tool for researchers and educators that is easy to use and modify" [51]

$$\tilde{g}(x,t) = S_{\text{bus}}(t) + S_d(t) - C_g S_g(t) = 0 \tag{6.1}$$

where $S_{\text{bus}}(t)$ is the matrix of complex power injections and is defined as follows:

$$S_{\text{bus}}(t) = V(t)I^*_{\text{bus}}(t) = V(t)Y^*_{\text{bus}}V(t)^* \tag{6.2}$$

$S_d = P_d + jQ_d$ is a vector of size $n_b \times 1$ and denotes the complex power load at all buses. The load values are given as input to the model. The vector of generator injections, $S_g = P_g + jQ_g$, is a $n_g \times 1$ vector. We need this vector to have the same size as S_d. Thus, a $n_b \times n_g$ generator connection matrix, C_g, is defined such that its $(ij)^{th}$ element is 1 if a generator is located at bus i and 0 otherwise. As a result, we get a $n_b \times 1$ vector of bus injections: $S_{g,\text{bus}} = C_g S_g$. Equation (6.1) is the mismatch between scheduled and calculated powers. For more information on the mismatch vector and the iterative solution process of the power balance equations, see section 3.1. The matrix of scheduled apparent power injected to system buses is determined from equation (6.2), whereas the calculated injected powers, are determined from the built-in MATPOWER function `makeSbus`. The function `makeSbus` create a matrix of injected powers by summing up the injected generation and injected load at each bus.

When determining the non-linear inequality constraints, representing the limits on apparent power flow, we utilize the following relation.

$$\tilde{h}(x,t) = \begin{bmatrix} h(t)^f \\ h(t)^t \end{bmatrix} = \begin{bmatrix} S^{f^*}S^f - S^2_{\max} \\ S^{t^*}S^t - S^2_{\max} \end{bmatrix} \leqslant 0 \tag{6.3}$$

Where S^f and S^t are the complex powers injected at the "from"- and "to" bus, respectively, and $S^2_{\max}$ is the squared vector of apparent power flow limit.

To summarize, when evaluating the nonlinear constraints of the model, namely the power balance equations and the branch flow limit, here expressed as $\tilde{g}(x,t)$ and $\tilde{h}(x,t)$, the MATPOWER built in function `makeSbus` is adopted. In addition parts of the proposed solution process is influenced by how the constraints are handled in the MATPOWER function `opf_consfcn`. In MATPOWER, `opf_consfcn`, is the function evaluating the nonlinear constraints and their Jacobian when calculating AC optimal power flow.

Chapter 7

Case Studies

This chapter presents the results generated during the thesis work along with a brief discussion of the observations. For all case studies, the model shown in section 5.1.4, is implemented in MATLAB where the `fmincon` solver in the Optimization Toolbox with default interior point algorithm is used to solve the multi-period AC OPF problem.

The main focus of this work is a pedagogical presentation of the theoretical framework and methodological procedure of multi-period AC OPF. Therefore the code is applied to reasonably simple systems. The overall purpose of the case study is to illustrate some of the analyses that can be performed by the proposed method.

7.1 3-Bus Test System

This section contains the results from applying the multi-period AC OPF model to the 3-bus test system introduced in section 5.3. The time horizon consist of four time-steps, $T = 4$ and $\Delta t = 1$. Information about generation and load is given at four points in time.

The results from the simulation aim to illustrate how the operation strategy of energy storage is strongly dependent on the mathematical formulation of the objective function. Three different formulations of a cost-minimizing objective function are introduced, as shown below. The system is simulated for the three cases, and the results are discussed.

(a) Constant cost-function

$$\min \sum_{t=1}^{T} bP_1(t) = \sum_{t=1}^{T} 400P_1(t) \tag{7.1}$$

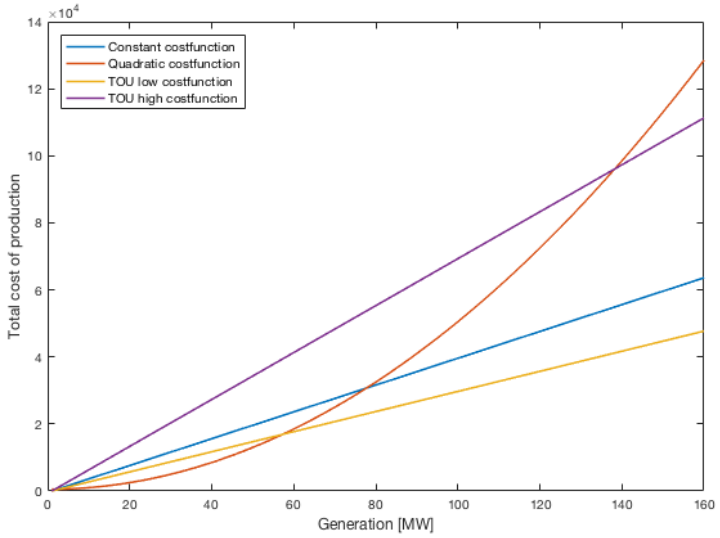

Figure 7.1: Objective functions plotted against power generation on the x-axis

(b) Quadratic cost-function

$$\min \sum_{t=1}^{T} aP_1^2(t) + bP_1(t) + c = \sum_{t=1}^{T} 500P_1^2(t) + 10P_1(t) + 5 \tag{7.2}$$

(c) Time-varying cost-function

$$\min \sum_{t=1}^{T} b_i P_1(t) = 300P_1(1) + 700P_1(2) + 300P_1(3) + 700P_1(4) \tag{7.3}$$

The parameter values are chosen for an illustrative purpose. In figure 7.1 the cost-functions are plotted against generation on the x-axis. The y-axis gives the total generation cost, such that the cost of generation per MW is given by dividing the y-value on the x-value.

The blue curve is depicting the constant cost-function (a). The marginal cost of production is constant for all values of generation throughout the entire simulation period. The quadratic cost-function (b) is illustrated by the red curve and is also represented by the same curve through the whole simulation period. In contrary to (a), the marginal cost of production is rising in line with an increasing generation. Thus, the cost per MW production is more expensive when the demand is high. The third alternative of formulating the objective function, the time-varying cost-function (c), is illustrated by the purple and yellow curve. As seen from the mathematical formulation of the function 7.3, the production cost is dependent on the time of production.

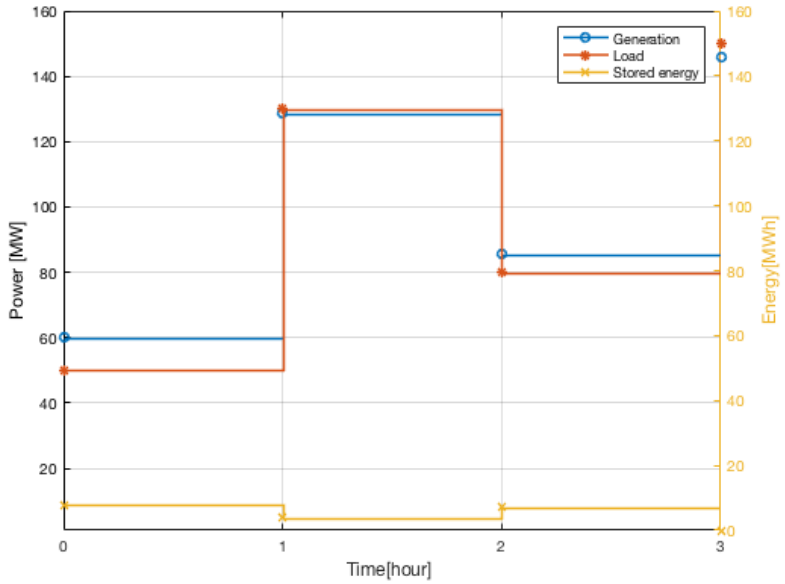

Figure 7.2: Operation strategy with objective function formulated as a minimizing constant cost-function (a)

The results from the three simulations are illustrated in figure 7.2, 7.3 and 7.4. The blue curve is depicting the generation from the generator connected to bus 1, the red curve is illustrating the load pattern and the yellow curve is showing the amount of energy stored in the storage in each period. Note that the load at $t = 3$ is increasing to $150MW$, this is affecting the operation schedule.

The value of input parameters is given at a discrete point in time. Thus, taking the generation as an example. When simulating over a time horizon of four moments $t = [0, 1, 2, 3]$, four values of generation are given as input. When plotting these values, the amount of generation at one step is assumed to be constant until the next step is reached.

Figure 7.2 show the result from the simulation when minimizing a constant cost-function. It is seen from the graph that the battery is barely being utilized. Studying the results of simulation when minimizing a quadratic function, depicted in figure 7.3, it is observed that the storage is being utilized considerably more. In this case, the optimal operation strategy is to charge the battery when the demand is low and dispatch this energy when the load demand is higher. This is due to the marginal cost of power being greater when the production volume is increasing. Thus, by utilizing the battery storage, the overall generation profile flattens out, and the cost of generation is minimized. Figure 7.4 depict the results from simulation when the objective function is formulated as a time-varying cost-function. From the formulation of the objective

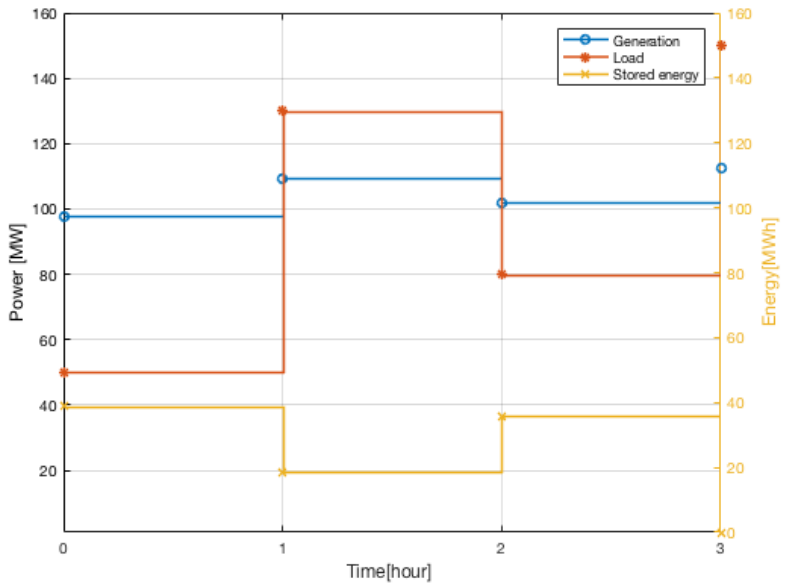

Figure 7.3: Operation strategy with objective function formulated as a minimizing quadratic cost-function (b)

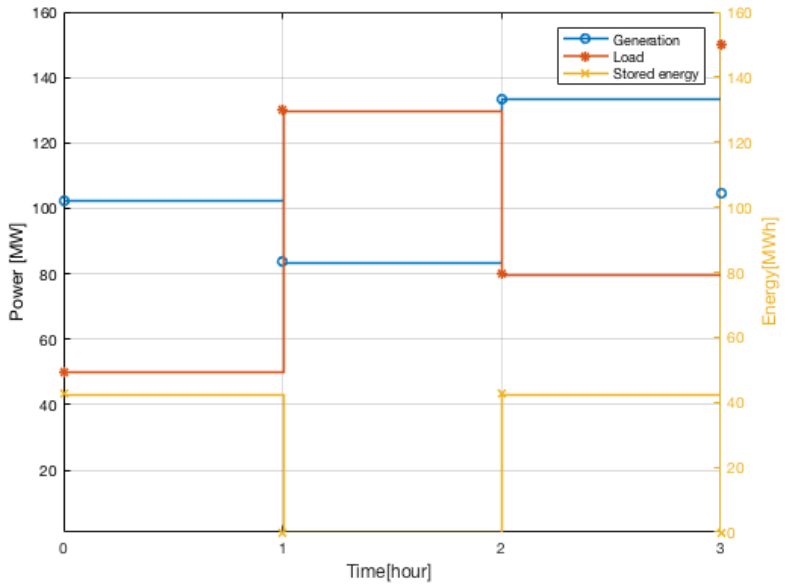

Figure 7.4: Operation strategy with objective function formulated as a minimizing time-varying cost-function (c)

function in equation 7.3, it is noticeable that two cost-levels are illustrating that the price of electricity is higher when the demand is high. Within the range of power demand (50MW-150MW), the cost of power generation given by the quadratic function is located between the curve describing the high cost and low cost of generation from the time-varying representation of the objective function. This is visible from figure 7.1. Thus, there is an even higher intensive for the model to charge the battery during valley-periods and discharge power during periods of peak load. From the plotting, it is observable that the generation between time-step 2 and 3 is higher than in the two other cases. The great step in the generation is due to the peak load occurring at $t = 3$ during a high-cost period. Thus, the model wants to store energy during a low-cost period ($t = 2 \rightarrow t = 3$) such that the stored energy can be dispatched when the cost of generation is expensive.

7.1.1 Discussion

The multi-period AC OPF model was applied to the 3-bus test system with the purpose of providing a simple illustration of how the energy storage unit affect the energy flow in the system. The values of storage energy capacity and power capacity were chosen such that it would not be a binding constraint. The overall results from the simulation are as expected: Since the operation cost of the battery is zero, the storage is charged during valley hours and discharged during peak hours. Thus, installing the battery results in a more flattened generation profile. The outcome of studying different cost-minimizing objective functions resulted mainly in two observations. Firstly, the output from OPF analysis is greatly dependent on the formulation of the objective function. Thus, when creating a multi-period AC OPF, or any other optimization model, thoughtful and realistic presentation of the objective function is of great importance. Secondly, when examining the differences in the operation schedule of the storage, we can conclude that there is a greater intensity for utilizing the energy storage when there is a greater variation in production cost.

7.2 Modified IEEE 9-Bus System

This section contains the results from applying the multi-period AC OPF model to the 9-bus test system introduced in section 6.2. The system is studied over a 24-hour time horizon split

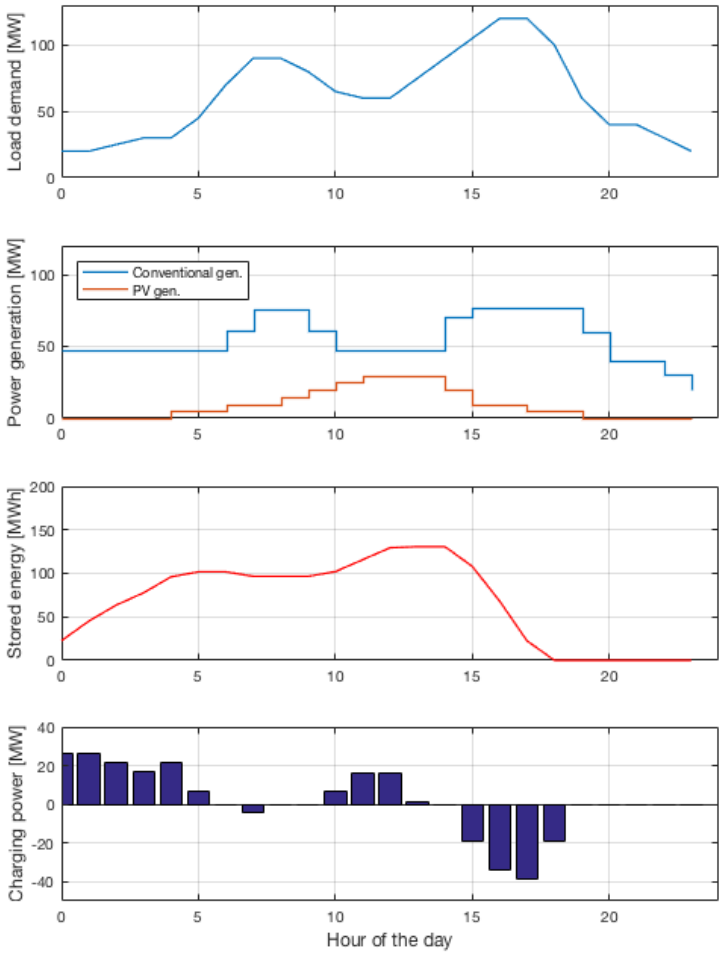

Figure 7.5: Results from the multi-period AC OPF simulation depicting hourly operation strategy

up into 1-hour time-steps. Figure 7.5 is depicting the optimal hourly operation strategy of the system. The upper graph is illustrating the total system load profile, which is given as input data to the model. The second graph is presenting the total power generation. The PV generation is deterministic and given to the model as input value while the value of total production from conventional generators is derived during the optimization procedure and are thus outputs from the model. The third graph is providing energy stored in the battery at all times. The bottom graph is depicting the charging/discharging schedule of energy storage. Positive values represent that the storage is being charged i.e. demanding power from the grid, while negative values mean that the storage is discharging i.e. delivering power to the grid.

When analyzing the results, we start by noticing that the load profile is following a curve

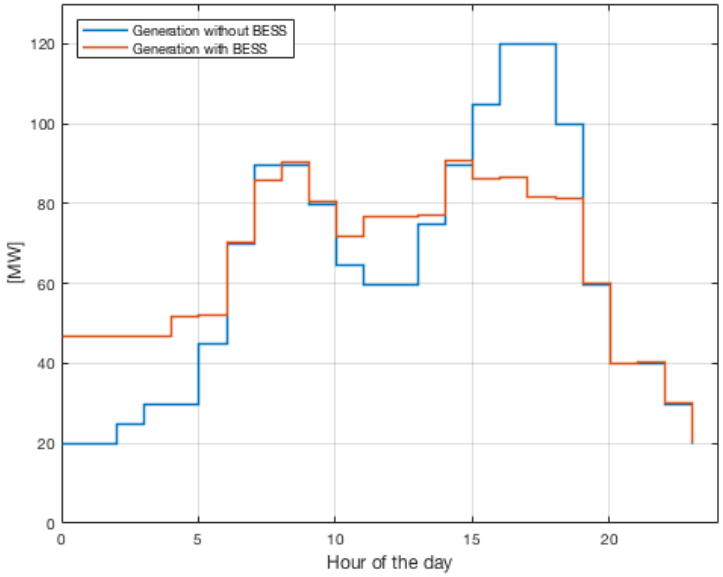

Figure 7.6: Hour by hour generation with and without BESS installed in the system

with two peaks, one in the morning and one in the afternoon, as predetermined. The peak in the morning is mostly covered by power from conventional generators, with a small power contribution from PV generation and storage. The peak in the afternoon is to a greater extent covered by power from the energy storage. Energy is stored in the battery during the day when production exceeds demand. The objective function is formulated as a quadratic function. Thus the model chose to generate more power than necessary during low demand and store the excess energy, as explained more in detail in the 3-bus example. Besides, energy is being stored when the PV generation is at its maximum. During the peak demand in the afternoon, the battery act as a generator such that conventional generators can generate less than it would have to if the battery was not installed.

Figure 7.6 clearly illustrates how energy storage can be utilized in peak shaving and valley filling. The figure consists of two plots, one depicting the total load demand in the system and the other showing the required generation from conventional- and PV generators when a BESS is included in the system. In a power system with no possibility of storing energy, the power generation must meet the demand at all times. Thus, the plot describing the generation profile must be identical to the load profile. From the simple scenario in this case study, not having energy stored, would result in both higher peak- and lower valley values of a generation.

7.2.1 Discussion

In the above case-study, the multi-period AC OPF model was applied to a modified version of the IEEE 9-bus system, including energy storage and PV generation. The primary goal of implementation was to make sure the code was able to find a feasible solution when studying such a system. Furthermore, the purpose of the study was to simulate a typical operation schedule when both renewable generation and storage is deployed in the grid. And moreover, it illustrates that the installation of energy storage can help reduce the strain on the grid during peak-hours and facilitate for higher penetration of renewable generation. As the input-values and grid characteristics do not represent a typical distribution system, the study cannot contribute to any concrete recommendations. However, the study has proven that the developed multi-period AC OPF model and methodology can be adopted in the optimization of power systems, including renewable generation and energy storage.

7.3 Radial 9-Bus System

This section contains the results from applying the multi-period AC OPF model to the radial version of the 9-bus test system introduced in section 6.3. The system is studied over a 24-hour time horizon split up into 1-hour time-steps. We are studying the results from implementing two different objective functions: a quadratic cost function and a time-variable cost-function based on values from Nordpool [18].

7.3.1 Case: Quadratic Cost-Function

Figure 7.7 depict the results from the simulations when the objective is formulated as a minimizing quadratic cost-function. By inspection of the plot describing the energy stored, it is noticeable that the storage is being charged and discharged twice during the simulation horizon. By also taking into consideration the curve describing the load pattern, it is apparent that the storage is being charged in the time-period before a peak load. This conforms with the result of studying the 3-bus system with a quadratic objective function. The model generates more power than needed when demand is low such that the overall cost is decreased.

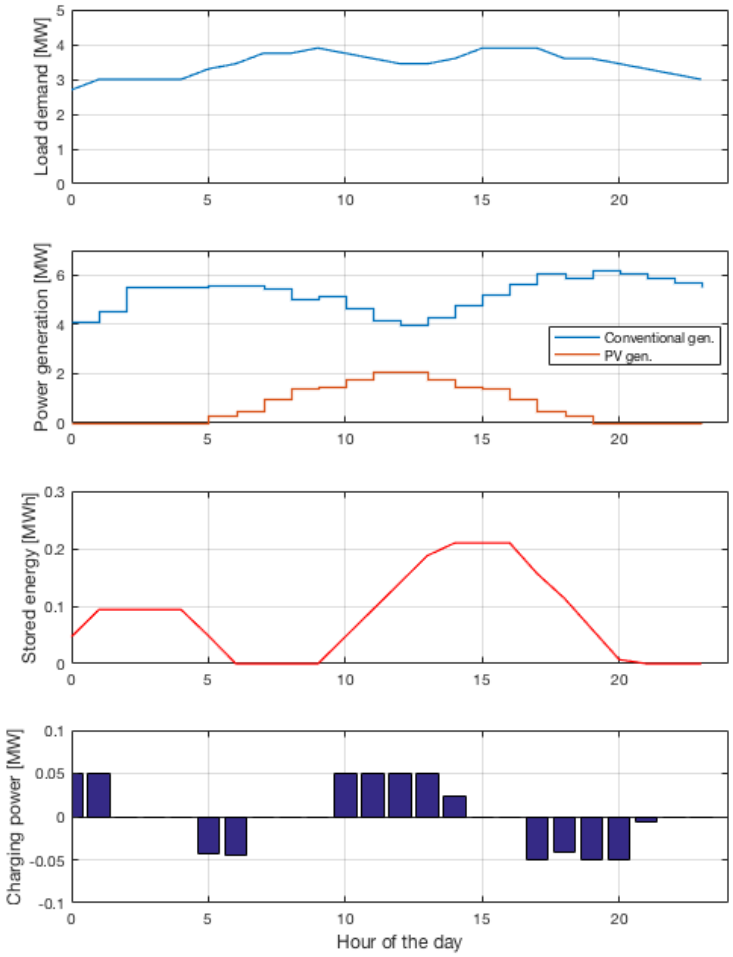

Figure 7.7: Results from the multi-period AC OPF simulation depicting hourly operation strategy with quadratic cost-function

7.3.2 Case: Time-Variable Cost-Function

This section presents the results from applying the multi-period AC OPF model to the 9-bus radial system when the objective function is formulated as a time-varying cost function. The price data is obtained from NorPool and represents the spot price of electricity [NOK/MWh] for Oslo May 24th, 2019 [18]. Investigating the results given in figure 7.8, it is observable that the varying spot price is the driving force for charging and discharging the battery. The storage is charged during the night when the cost is low and discharged during the morning-peak when both demand and costs are high. During mid-day, when the PV generation is at its maximum, the conventional generation is decreasing such that the PV generation contributes to covering the load demand at the current time-step.

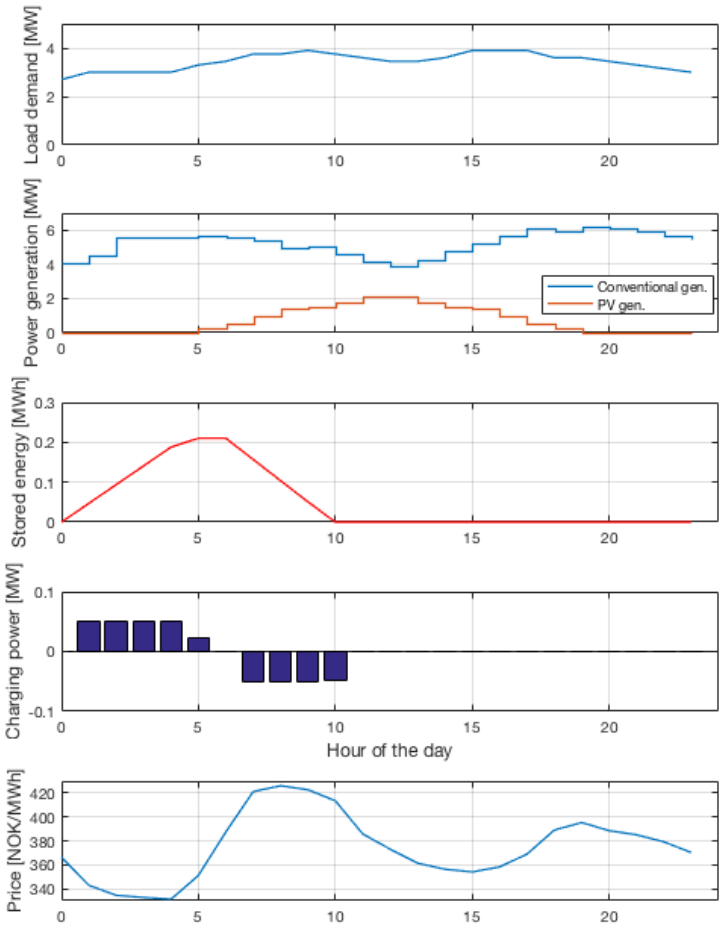

Figure 7.8: Results from the multi-period AC OPF simulation depicting hourly operation strategy with time-variable cost-function. Spot prices for Oslo, May 24th 2019. Data retrieved from NordPool [18]

7.3.3 Discussion

From the two above simulations, and as stated earlier, it is observable that the formulation of the objective function has a significant impact on the simulation results. When simulating based on a quadratic cost-function, the results match the expected outcome. While, when spot prices represent the cost-function, the storage is not being utilized in the middle of the day. This could be investigated further in future work.

7.4 Discussion of Case Studies

In the preceding sections, case studies have been performed on various test systems to demonstrate the performance of the multi-period AC OPF structure presented in this thesis. The results show that the implemented model can be successful in producing the optimal operation strategy for energy storage systems. It was observed through simulations that the implemented code did not manage to find a feasible solution for all systems, only cases that converged is included here. This is obvious a weakness of the code, and is discussed further in section 8.2.

The simulations manage to illustrate a few of the applications energy storage systems can provide when utilized as a flexible energy source. Firstly, it is shown that the battery can help reduce the strain on the grid during peak hours by contributing to peak-shaving and valley-filling, resulting in local energy balance. Furthermore, this operation can reduce the overall cost of generation. Secondly, if a decentralized generation is deployed in the grid, it is shown that the storage unit can facilitate a higher amount of renewable production.

In the multi-period AC OPF structure presented in this theses, several simplifications were made. Firstly, the load pattern and PV production are considered to be deterministic over the simulation horizon. The model presented assume that consumer demand can be predicted accurately in advance. The future load pattern will be defined by higher peaks and more uncertainty, making it even harder to predict. The PV production is also handed to the model as a foreknown input-value, which is a simplification as the generation is dependent on the stochasticity of solar irradiance. Secondly, in the modeling of battery storage, only active power is considered.

The next step of the case studies would have been to test the code on a distribution system of greater size with all parameter values according to a real distribution grid. Due to limitations in time, this was not done during the thesis work.

Chapter 8

Conclusion and Further Work

This chapter makes some concluding remarks about the work presented and its findings. It also suggests some areas of future research both in terms of methodology and application.

8.1 Conclusion

This thesis has studied the field of multi-period AC OPF within power system optimization. The ongoing transformation towards a power system characterized by a higher level of flexibility and complexity drives the need for finding new ways of analyzing the system. This work has particularly investigated the deployment of energy storage systems in the distribution grid. The BESS introduces interdependent couplings between the time-steps of the planning horizon, making it unfavorable to consider each time-step separately.

This thesis has aimed to provide the reader with a conceptual understanding of this state-of-art work from the perspective of pedagogical clarity. Thus, a significant part of the work has been spent on understanding the essential details of multi-period AC OPF formulation and modeling. A literature survey has also been conducted to elucidate the scope of research done on the relevant subject. The survey investigates five papers focusing on multi-period AC OPF problems when including energy storage in the power system. The survey demonstrates that even within this narrow field of study, there has been published a vast amount of work focusing on different aspects of the challenge and adopting various methods and tools for solving the problem.

Besides the emphasis that has been laid on providing pedagogical clarity of the methodolog-

ical theory, a multi-period AC OPF model has been built and tested on various systems. The model is written in MATLAB and solved using `fmincon`. In chapter 5, the details of creating a mathematical model is presented, and a demonstration of the step-by-step implementation is provided.

The scripts were tested on three systems: a 3-bus system, a modified version of the IEEE 9-bus and a radial 9-bus system created with the IEEE 9-bus as a base. As previously stated, the main focus of this work has been to provide a pedagogical presentation of the theoretical framework and methodological procedure of multi-period AC OPF.

Thus, the case studies have been kept simple and illustrative. The methodology was applied to small test-systems, to illustrate the characteristics of system operation strategy when deploying energy storage. Another purpose of the case studies was to show different analyses that can be performed by using a multi-period AC OPF.

Studying the results from the 3-bus case, it was observed that the optimal operation strategy is to charge the battery when demand is low, and dispatch the energy when demand is greater. Different formulations of a cost-minimizing objective function were implemented to illustrate how the operation strategy of the battery is strongly dependent on the formulation of the objective function.

The two 9-bus systems have distributed generation installed in the form of a deterministic PV generation. When applying the implemented multi-period AC OPF model to the 9-bus IEEE test system, the operation strategy over a 24-hour horizon was investigated. It was observed that energy was stored in the battery when production exceeds demand. The stored energy is dispatched at a later time when demand is higher and contribute to cover the peak load in the afternoon. The case study illustrates that the installation of energy storage can help reduce the strain on the grid during peak-hours and facilitate for higher penetration of renewable generation.

The radial 9-bus system was implemented to make sure that the developed code also works on systems of radial structure. The input parameters were scaled down to represent typical distribution system values with the ambition of obtaining more realistic results. Two mathematical formulations of the objective function and their impact on the charging/discharging schedule were studied. It was observed that the formulation of the objective function greatly influences the system operation strategy. Hence, the result emphasizes the importance of a thoughtful

construction of the mathematical system model.

The main focus of this thesis has not been to develop and execute a case study resulting in a concrete recommendation. But rather to provide a pedagogical presentation of the theoretical framework and the methodological procedure of multi-period AC OPF, such that this thesis can form the basis for further research on the subject. Therefore, it is difficult to state a definite conclusion. Nevertheless, multi-period AC OPF has proven to be a powerful tool in power system analyzing when optimization over a time horizon is favorable.

8.2 Further Work

There are several aspects of this thesis that can form the basis for further research, both in terms of methodology and application.

In terms of improvements in methodology, some further work may consist of creating a universal code that can work on any system sizes, as the codes presented in this thesis are created for a unique system.

During the thesis work, multiple variations of the test systems have been implemented. In some cases, the solver did not find a feasible solution. Future research could examine this weakens. The `fmincon` solver includes several solution algorithms, one possible extension of the work would be to apply a different algorithm such as sequential quadratic programming or active set. Another interesting point could be to solve the multi-period AC OPF by calling another solver (e.g., `knitro` or `ipopt`).

The case studies in this thesis are studying the effect of varying the mathematical formulations of a cost-minimizing objective function. Further research may expand the work by looking into other objectives like minimization of system losses.

The most obvious suggestion for future work within the application would be to apply the suggested multi-period AC OPF to a system consisting of real distribution system values providing a good basis for further research.

In future work, it would be interesting to include a more detailed load modeling e.g separate load curves for individual households or study the stochasticity related to charging of the increasing EV fleet.

Within the field of uncertainty modeling, it would also be interesting to investigate the possibility of demand response as a flexible resource. Taking into account stochasticity and forecast uncertainty in solar irradiance could also be an interesting direction for further work.

Bibliography

[1] Z. Wang, J. Zhong, D. Chen, Y. Lu, and K. Men, "A multi-period optimal power flow model including battery energy storage," *IEEE Power and Energy Society General Meeting*, pp. 1–5, 2013.

[2] C. K. Das, O. Bass, G. Kothapalli, T. S. Mahmoud, and D. Habibi, "Overview of energy storage systems in distribution networks: Placement, sizing, operation, and power quality," *Renewable and Sustainable Energy Reviews*, vol. 91, no. March, pp. 1205–1230, 2018.

[3] H. Abdi, S. D. Beigvand, and M. L. Scala, "A review of optimal power flow studies applied to smart grids and microgrids," 2017.

[4] I. B. Sperstad and H. Marthinsen, "Optimal power flow methods and their application to distribution systems with energy storage," *SINTEF Energy Research*, vol. [Report nu, 2016.

[5] English Wiktionary, "Your dictionary." `https://www.yourdictionary.com/intertemporal`. [Online; accessed 24-May-2019].

[6] H. Bindner, *Power Control for Wind Tur- bines in Weak Grids : Concepts Development*, vol. 1118. 1999.

[7] F. Meng, "A generalized optimal power flow program for distribution system analysis and operation with distributed energy resources and solid state transformers," 2014.

[8] A. Gavrilovic, "Ac/dc system strength as indicated by short circuit ratios," in *International Conference on AC and DC Power Transmission*, pp. 27–32, Sept 1991.

[9] M. Mahmud, M. Hossain, and H. Pota, "Analysis of voltage rise effect on distribution network with distributed generation," *IFAC Proceedings Volumes*, vol. 44, pp. 14796–14801, Jan 2011.

[10] H. Saadat, *Power System Analysis*. New York: PSA Publishing, 3rd ed., 2010.

[11] Norges vassdrags- og energidirektorat, "Forskrift om leveringskvalitet i kraftsystemet." `https://lovdata.no/dokument/SF/forskrift/2004-11-30-1557`, 2004. [Online; accessed 13-November-2018], [English: The Norwegian Water Resources and Energy Directorate, Regulation on Quality of Supply in the Electric Power Grid].

[12] IEA: International Energy Agency, "Solar PV." `https://www.iea.org/tcep/power/renewables/solar/`. [Online; accessed 8-December-2018].

[13] Multiconsult and Asplan Viak, "Solcellesystemer og sol i systemet," Mar 2018.

[14] DNV GL, "Batterier i distribusjonsnettet," tech. rep., NVE, 2018.

[15] E. Aguiar, R. Cardoso, C. Stein, J. Costa, and E. Carati, *Distributed Renewable Power Sources in Weak Grids — Analysis and Control*, ch. 9, pp. 200–225. Brazil: IntechOpen, 2016.

[16] C. L. Masters, "Voltage rise: the big issue when connecting embedded generation to long 11 kv overhead lines," *Power Engineering Journal*, vol. 16, pp. 5–12, Feb 2002.

[17] R. Secretariat, "Renewables 2018 global status report," *REN21 Renewable Energy Policy Network for the 21st Century*, Paris, 2018.

[18] Nord Pool AS, "Market data." `https://www.nordpoolgroup.com/Market-data1/Dayahead/Area-Prices/ALL1/Hourly/?view=table`. [Online; accessed 24-May-2019].

[19] THEMA Consulting Group, *Teoretisk tilnærming til en markedsløsning for lokal fleksibilitet. Konsulentrapport utarbeidet for NVE.* No. 978, 2016.

[20] M. Nick, R. Cherkaoui, and M. Paolone, "Optimal siting and sizing of distributed energy storage systems via alternating direction method of multipliers," *International Journal of Electrical Power Energy Systems*, vol. 72, pp. 33–19, November 2015.

[21] C. Das, O. Bass, G. Kothapalli, M. Thair, and D. Habibi, "Overview of energy storage systems in distribution networks: Placement, sizing, operation, and power quality," *Renewable and Sustainable Energy Reviews*, vol. 91, pp. 1205–1230, 2018.

[22] M. Z. Degefa, H. Sæle, J. A. Foosnaes, and E. Thorshaug, "Seasonally variant deployment of electric battery storage systems in active distribution networks," *CIRED - Open Access Proceedings Journal*, vol. 2017, no. 1, pp. 1975–1979, 2017.

[23] N. Etherden and M. H. J. Bollen, "Dimensioning of energy storage for increased integration of wind power," *IEEE Transactions on Sustainable Energy*, vol. 4, pp. 546–553, July 2013.

[24] N. Meyer-Huebner, M. Haas, M. Uhrig, M. Suriyah, and T. Leibfried, "Dynamic optimal power flow for dimensioning and operating quarter based storage in low voltage grids," in *2017 IEEE PES Innovative Smart Grid Technologies Conference Europe (ISGT-Europe)*, pp. 1–6, Sept 2017.

[25] J. Glover, M. Samra, and T. Overbye, *Power System Analysis and Design*. Stamford, USA: Cengage Learning, 5th ed., 2012.

[26] S. Frank and S. Rebennack, "An introduction to optimal power flow: Theory, formulation, and examples," *IIE Transactions (Institute of Industrial Engineers)*, vol. 48, no. 12, pp. 1172–1197, 2016.

[27] M. Farivar and S. H. Low, "Branch flow model: Relaxations and convexification-part i," *IEEE Transactions on Power Systems*, vol. 28, no. 3, pp. 2554–2564, 2013.

[28] H. Abdi, S. D. Beigvand, and M. L. Scala, "A review of optimal power flow studies applied to smart grids and microgrids," 2017.

[29] A. Sallam and O. Malik, *Power System Stability - Modelling, Analysis and Control*. Institution of Engineering and Technology, 1st ed., 2015.

[30] H. Glavitsch and R. Bacher, "Optimal power flow problem algorithms," *Swiss Federal Institute of Technology*, 1991.

[31] S. Chatzivasileiadis, "Lecture Notes on Optimal Power Flow (OPF)," no. September, 2018.

[32] S. Gill, I. Kockar, and G. W. Ault, "Dynamic optimal power flow for active distribution networks," *IEEE Transactions on Power Systems*, vol. 29, no. 1, pp. 121–131, 2014.

[33] S. Zaferanlouei, M. Korpaås, J. Aghaei, H. Farahmand, and N. Hashemipour, "Computational efficiency assessment of multi-period AC optimal power flow including energy storage systems," *2018 International Conference on Smart Energy Systems and Technologies, SEST 2018 - Proceedings*, 2018.

[34] A. J. Lamadrid, T. D. Mount, and R. J. Thomas, "Scheduling of Energy Storage Systems with geographically distributed renewables," *Proceedings - 9th IEEE International Symposium on Parallel and Distributed Processing with Applications Workshops, ISPAW 2011 - ICASE 2011, SGH 2011, GSDP 2011*, pp. 85–90, 2011.

[35] I. Sperstad, "Batterier som fleksibel ressurs i distribusjonsnettet," Trondheim, 2018. Power Point from WP3/5-workshop, CINELDI.

[36] J. Zhang, "on Distributed Optimization Methods for Solving Optimal Power Flow Problem Over Electricity Grids," no. August, 2016.

[37] MathWorks, "Constrained nonlinear optimization algorithms." `https://ch.mathworks.com/help/optim/ug/constrained-nonlinear-optimization-algorithms.html#brnpd5f`. [Online; accessed 25-Mars-2019].

[38] J. Nocedal and S. Wright, *Numerical Optimization*. New York, USA: Springer, 1999.

[39] J. Zhu, *Optimization of Power System Operation*. Hoboken, New Jersey: John Wiley Sons, 2009.

[40] A. C. Mary B. Cain, Richard P. O'Neill, "Optimal Power Flow and Formulation," no. December, pp. 1–36, 2012.

[41] N. T. Nguyen, D. D. Le, C. Bovo, and A. Berizzi, "Optimal Power Flow with energy storage systems: Single-period model vs. multi-period model," *2015 IEEE Eindhoven PowerTech, PowerTech 2015*, pp. 1–6, 2015.

[42] X. Zhang, F. Gao, X. Lv, H. Lv, Q. Tian, J. Ma, W. Yin, and J. Dong, "Line loss reduction with distributed energy storage systems," *2012 IEEE Innovative Smart Grid Technologies - Asia, ISGT Asia 2012*, pp. 1–4, 2012.

[43] H. M. Costa, J. Sumaili, A. G. Madureira, and C. Gouveia, "A multi-temporal optimal power flow for managing storage and demand flexibility in LV networks," *2017 IEEE Manchester PowerTech, Powertech 2017*, no. 645963, 2017.

[44] F. Habashi, "Reactive metals and the periodic table," *Light Metals 1992*, pp. 1279–1286, 1992.

[45] H. Pandžić and V. Bobanac, "An accurate charging model of battery energy storage," *IEEE Transactions on Power Systems*, vol. 34, no. 2, pp. 1416–1426, 2019.

[46] J. Xie, J. Ma, and K. Bai, "Enhanced Coulomb Counting Method for State-of-Charge Estimation of Lithium-ion Batteries based on Peukert's Law and Coulombic Efficiency," vol. 18, no. 3, pp. 1–13, 2018.

[47] C. Mathworks, "Optimization Toolbox ™ User ' s Guide R 2018 b," 2018.

[48] P.S.R. Murty, *Power System Analysis*. Elsevier Ltd, 2end ed., 2017.

[49] F. K. Ariyo, "Electrical Network Reduction for Load Flow and Short-Circuit Calculations Using Power Factory Software," *American Journal of Electrical Power and Energy Systems*, vol. 2, no. 1, p. 1, 2013.

[50] Tesla 2018, "Tesla powerpack." `https://www.tesla.com/en_AU/powerpack?redirect=no`. [Online; accessed 29-May-2019].

[51] R. D. Zimmerman, C. E. Murillo-Sánchez, *et al.*, "Matpower." `http://www.pserc.cornell.edu/matpower/`. [Online; accessed 11-May-2019].

[52] R. D. Zimmerman and C. E. Murillo-Sánchez, "Matpower Optimal Scheduling Tool MOST 1.0 User's Manual," 2016.

Appendix A

Formula: Voltage drop

Referring to the work in [9] and fig. 2.1. The voltage at sending end is given

$$\hat{V_{\mathrm{S}}} = \hat{V_{\mathrm{R}}} + \hat{I}(R + jX) \tag{A.1}$$

The power supplied from up-grid, can be written as

$$P + jQ = \hat{V_{\mathrm{S}}}\hat{I}^{*} \tag{A.2}$$

Resulting in a current flowing from sending to receiving end given by

$$\hat{I} = \frac{P - jQ}{\hat{V_{\mathrm{S}}}} \tag{A.3}$$

By using A.1 and A.3, we get an expressing for the voltage at sending end

$$\hat{V_{\mathrm{S}}} = \hat{V_{\mathrm{R}}} + \frac{P - jQ}{\hat{V_{\mathrm{S}}}}(R + jX) = \hat{V_{\mathrm{R}}} + \frac{RP + XQ}{\hat{V_{\mathrm{S}}}} + j\frac{XP - RQ}{\hat{V_{\mathrm{S}}}} \tag{A.4}$$

Hence, the voltage drop can be written as

$$\hat{V_{\mathrm{S}}} - \hat{V_{\mathrm{R}}} = \Delta\hat{V} = \frac{RP + XQ}{\hat{V_{\mathrm{S}}}} + j\frac{XP - RQ}{\hat{V_{\mathrm{S}}}} \tag{A.5}$$

Assuming the angle between sending and receiving end to be small, the voltage drop can be approximated to the real part of the equation, resulting in

$$\Delta V \approx \frac{RP + XQ}{\hat{V_{\mathrm{S}}}} \tag{A.6}$$

Appendix B

MATLAB code

The code for the 3-bus test system is shown below. For the two 9-bus cases, the methodical layout is equal. Due to a larger optimization-vector, some modifications are completed.

B.1 3-Bus Test System

`main3bus.m`

```
clear;
close all
clc
%% Load power system data
LoadData3bus

%% Variable bounds
ub = zeros(numvar,1);
lb = zeros(numvar,1);

% Bounds on voltage angle
ub(1)= Deltamax(1);
lb(1)= Deltamin(1);
ub(2)= Deltamax(2);
lb(2)= Deltamin(2);
ub(3)= Deltamax(3);
lb(3)= Deltamin(3);
```

```
% Bounds on voltage magnitude
ub(4)= Vmax(1);
lb(4)= Vmin(1);
ub(5)= Vmax(2);
lb(5)= Vmin(2);
ub(6)= Vmax(3);
lb(6)= Vmin(3);

% Bounds on real power generation
ub(7)= Pgmax(1);
lb(7)= Pgmin(1);

% Bounds on reactive power generation
ub(9)= Qgmax(1);
lb(9)= Qgmin(1);
ub(10)= Qgmax(2);
lb(10)= Qgmin(2);

% Bounds on energy stored
ub(8) = SOCmax;
lb(8) = SOCmin;

% Bonds on charging/discharging power
ub(11) = 0.5;
lb(11) = 0;
ub(12) = 0.5;
lb(12) = 0;

%% Initial guess
x0 = lb+(ub-lb)/2;
    x0(isnan(x0))=0;

%% multi-period expansion of vectors
X0 = zeros(T*numvar,1);
Lb = zeros(T*numvar,1);
Ub = zeros(T*numvar,1);
```

```
j=1;
    for i=1:size(Pd,2)
        X0(j:i*numvar) = x0;
        Lb(j:i*numvar) = lb;
        Ub(j:i*numvar) = ub;

        j=j+numvar;
    end

%% Linear constraints: FOR A THREE BUS SYSTEM WITH T=3
Aeq = zeros(T,T*numvar);
beq = zeros(T,1);
Aeq_s = zeros(1,2*12);

beq(1) = SOC0; %Given in loadData
Aeq(1,8) =  1;
Aeq(1,11) = -0.85;
Aeq(1,12) = 1/0.85;

Aeq_s(1,20) = 1;
Aeq_s(1,8) = -1;

% charge and discharge efficiencies
Aeq_s(1,23) = -0.85;
Aeq_s(1,24) =  0.85;

j=1;
for i = 2:T
    Aeq(i,j:i*numvar) = Aeq_s;
    j=j+numvar;
end

%% Non-linear constrains
ineq=@(x)nonlcon3(x,Pd,Qd,MVAbase, bus, gen, branch, numvar,...
numbus,numline, T);

%% Objective function. Choose one of three:
% 1) constant
```

```
% fun=@(x)(40000*x(7) +40000*x(19) + 40000*x(31) + 40000*x(43));
% 2) quadratic
fun=@(x)(500 + 10*x(7)*MVAbase + 5*(x(7)*MVAbase)^2)...
+ (500 + 10*x(19)*MVAbase + 5*(x(19)*MVAbase)^2)...
+ (500 + 10*x(31)*MVAbase + 5*(x(31)*MVAbase)^2)...
+ (500 + 10*x(43)*MVAbase + 5*(x(43)*MVAbase)^2);
% 3) time-varying
%fun=@(x)(30000*x(7) + 70000*x(19) + 30000*x(31) + 70000*x(43));

%% Set Fmincon options
options = optimoptions('fmincon','Display','iter-detailed','MaxIter',60000,...
    'MaxFunEvals',600000,'TolCon',1e-10,'TolX',1e-12);

%% Run Optimization
[x_new] = fmincon(fun,X0,[],[],Aeq,beq,Lb,Ub,ineq,options);

%%  update control variable values
scale = zeros(numbus,1);
State_ofC = zeros(1,length(x_new)/numvar);
charge    = zeros(1,length(x_new)/numvar);
discharge = zeros(1,length(x_new)/numvar);
gen1      = zeros(1,length(x_new)/numvar);
Ploa3     = zeros(1,length(x_new)/numvar);

    for i=1:length(x_new)/numvar
        State_ofC(i)= x_new(8+(i-1)*12)*MVAbase;
        charge(i)=x_new(11+(i-1)*12)*MVAbase;
        discharge(i)=x_new(12+(i-1)*12)*MVAbase;
        gen1(i)=x_new(7+(i-1)*12)*MVAbase;
        Ploa3(i)=Pd(3,i);

    end

%% Plot results
% LOADPROFILE
figure(1)
stairs(Ploa3,'LineWidth',1.5, 'Marker', '*')
grid on
```

```
ylabel('Load [MW]', 'FontSize',12)
xlabel('Time [hour]','FontSize',12)
xlim([1 4]);
ylim([0 160]);
xticks([1 2 3 4]);
xticklabels({'0','1','2','3'});


% RESULTS
figure(2)
stairs(gen1, 'LineWidth',1.5, 'Marker', 'o');
hold on
stairs(Ploa3, 'LineWidth',1.5, 'Marker', '*');
ylim([1 160]);
xlim([1 5]);
xticks([1 2 3 4]);
xticklabels({'0','1','2','3'});
ylabel('Power [MW]', 'FontSize',12)
xlabel('Time[hour] ','FontSize',12)
yyaxis right
ylabel('Energy[MWh]', 'FontSize',12)
ylim([0 160]);
stairs(State_ofC,'LineWidth',1.5, 'Marker', 'x');
legend('Generation','Load','Stored energy')
grid on
```

LoadData3bus.m

```
%% Loading data, reading from file and creating Ybus
%% System input parameters

%Total number of variables in 1 hour for 3 bus system
% 1 theta1
% 2 theta2
% 3 theta3
% 4 V_1
% 5 V_2
```

```
% 6 V_3
% 7 P_1
% 8 SOC(1)
% 9 Q_1
% 10 Q_2
% 11 Pch_1
% 12 Pdis_1

%% Input Data File
[file,pathname] = uigetfile('*.xlsx*');
if (pathname == 0)
    error('You Must Select A Valid Data File')
end
S=file;          % Name of the File that we need to read

fprintf(' Case ID: %s \n',file);

bus = xlsread(S, 'BusData');
gen = xlsread(S, 'GenData');
branch = xlsread(S, 'BranchData');
Pd = xlsread(S, 'Pd');
Qd = xlsread(S, 'Qd');
[gencost_inputdata] = xlsread(S, 'GenCostData');

% Number of variables
numvar = 12;

% Set Apparent Power Base
MVAbase = 100;

% Number of planning periods
T = 4;

% Number of buses, lines and generators
numbus = 3;
numline = 3;
numgen = 2;
```

```
% Create vectors
Vmax = zeros(1,numbus);
Vmin = zeros(1,numbus);
Deltamax = zeros(1,numbus);
Deltamin = zeros(1,numbus);
Pgmax = zeros(1,numgen);
Pgmin = zeros(1,numgen);
Qgmax = zeros(1,numgen);
Qgmin = zeros(1,numgen);

% Storage
SOCmax = 3;
SOCmin = 0;
SOC0 = 0;

% Get values from Excel
for igen = 1:numgen
   Pgmax(igen) = gen(igen,9)/MVAbase;
   Pgmin(igen) = gen(igen,10)/MVAbase;
   Qgmax(igen) = gen(igen,4)/MVAbase;
   Qgmin(igen) = gen(igen,5)/MVAbase;
end

for ibus = 1:numbus
   Vmax(ibus) = bus(ibus,12);
   Vmin(ibus) = bus(ibus,13);
   Deltamax(ibus) = bus(ibus,14)*pi/180;
   Deltamin(ibus) = bus(ibus,15)*pi/180;
end
```

nonlcon.m

```
function [c, ceq]= nonlcon3(x,Pd,Qd,MVAbase, bus, gen,...
branch, numvar, numbus,numline, T)
%% build admittance matrices
[Ybus, Yf, Yt] = makeYbus(MVAbase, bus, branch);
```

```
%% Max apparent power squared
S_max = (branch(:, 6)/MVAbase).^2;

%% Create non-linear constraints for all timesteps
ceq  = zeros(T*2*numbus,1); % P and Q PF-equations for all buses for all timesteps
c = zeros(T*2*numline,1);   %

j=1;
k=1;

for i = 1:T
    %% Preparations
    % Create vectors of variables for current time step i
    Va = x(1+(i-1)*numvar:3+(i-1)*numvar);
    Vm = x(4+(i-1)*numvar:6+(i-1)*numvar);
    Pg = x(7+(i-1)*numvar);
    Qg = x(9+(i-1)*numvar);
    Qg(2,1)=0;
    Pg(2,1)=x(12+(i-1)*numvar)- x(11+(i-1)*numvar);

    % put Pg & Qg (for current time step (i) back in gen(matrix)
    gen(:, 2) = Pg * MVAbase;  % active generation in MW
    gen(:, 3) = Qg * MVAbase;  % reactive generation in MVAr

    bus(:, 3) = Pd(:,i) ;  % active demand in MW
    bus(:, 4) = Qd(:,i) ;  % reactive demand in MVAr

    % Creating Sbus
    Sbus = makeSbus(MVAbase, bus, gen); %net injected power in p.u.

    %% Non-linear equality constraints - Power flow equations
    % Complex voltage rectangular form:
    V = Vm .* exp(1j * Va);
    % Mismatch vector: mis = S_sch - S_calc:
    mis = V .* conj(Ybus * V) - Sbus;

    g = [real(mis) imag(mis)];
    % active- and reactive power mismatch for all buses:
```

```
    % P_sch - P(V,delta) and Q_sch - Q(V, delta)

    ceq(j:length(g)*i,1) = g;
      j=j+length(g);

    %% Non-linear inequality constraints - Flow limits
    %(Assuming branch-limits in all lines)

    % Complex power injected at "from" bus (p.u.):
    Sf = V(branch(:, 1)) .* conj(Yf * V);
    % Complex power injected at "to" bus (p.u.):
    St = V(branch(:, 2)) .* conj(Yt * V);

    h = [ Sf .* conj(Sf) - S_max; %branch apparent power limits (from bus)
          St .* conj(St) - S_max ];%branch apparent power limits (to bus)

    c(k:i*length(h),1) = h;
    k = k+length(h);

end
end
```

Line Nyegaard

Multi-Period AC Optimal Power Flow for Distribution Systems with Energy Storage

NTNU
Norwegian University of
Science and Technology